Origin of the Excited-State Absorption Spectrum of Polythiophene

Ras Baizureen Roseli, Patrick C. Tapping, and Tak W. Kee*

Department of Chemistry, The University of Adelaide, South Australia 5005, Australia

E-mail: tak.kee@adelaide.edu.au
Phone: +61-8-8313-5039

Abstract

The excited states of conjugated polymers play a central role in their applications in organic solar photovoltaics. The delocalized excited states of conjugated polymers are short-lived ($\tau < 40$ fs) but are imperative in the photovoltaic properties of these materials. Photoexcitation of poly(3-hexylthiophene) (P3HT) induces an excited-state absorption band but the transitions that are involved are not well understood. In this work, calculations have been performed on P3HT analogues using nonlinear response time-dependent density functional theory to show that an increase in the oligomer length correlates with the dominance of the $S_1 \rightarrow S_3$ transition. Furthermore, the predicted transition energy shows an excellent agreement with experiment. The calculations also yielded results on intramolecular charge transfer in P3HT due to the $S_1 \rightarrow S_3$ transition, providing insight into the mechanism of exciton dissociation to form charge carriers.

Graphical TOC Entry

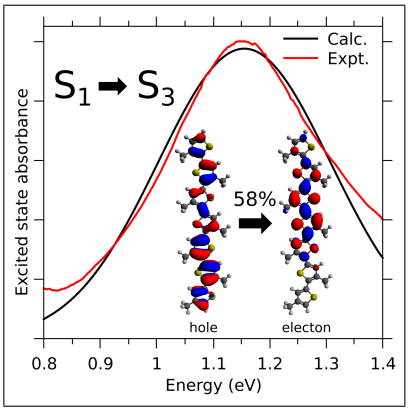

Keywords

P3HT, density functional theory, CAM-B3LYP, intramolecular charge transfer, exciton dissociation

Organic solar cells are photovoltaic devices consisting of electron donor and acceptor semiconducting materials with domain sizes of several nanometers.[1,2] Photoexcitation of either the donor or acceptor materials leads to the generation of molecular excitons, which subsequently migrate to the donor-acceptor heterojunction to undergo dissociation to form the hole and electron on the donor and acceptor, respectively.[3,4] Owing to strong Coulombic forces between the hole and electron, these species can still interact across the heterojunction. For organic solar cells that exhibit a significant efficiency, including those composed of a conjugated polymer (donor) and fullerene (acceptor), however, an effective charge separation at the heterojunction has been attributed to rapid diffusion of charges.[5,6] In 2012, a study by Bakulin et al. suggested that delocalized states of the exciton play a role in the effective formation of separated charges.[7] More recently, Gélinas et al. used a combination of ultrafast transient absorption spectroscopy and modeling to show that long-range charge separation requires rapid motion of the hole and electron away from the heterojunction through delocalized states of the exciton.[8] Using the excited-state absorption (ESA) band of blends of a number of conjugated polymers and fullerene, it was shown that electron-hole separation occurs with a time constant of <40 fs.[8] Although the ESA band of conjugated polymers is often used to reveal insight into the dynamics of excitons and separated charges, the physical nature of the absorption band, particularly the transitions that are involved, is insufficiently understood.

Polythiophenes are some of the most widely studied conjugated polymers in organic solar cells.[9] Poly(3-hexylthiophene) (P3HT), as shown in Figure 1, is one of the most studied conjugated polymers.[10,11] Phenyl-C_{61}-butyric acid methyl ester (PCBM) is typically used alongside P3HT as an electron acceptor in a bulk-heterojunction organic photovoltaic device.[12] Regioregular P3HT can aggregate due to face-to-face π–π stacking, resulting in crystallization and formation of nanofibers, which have long-range order.[13,14] The use of P3HT nanostructures in organic photovoltaics has led to an improved power conversion efficiency because of efficient exciton and hole transport.[15–19]

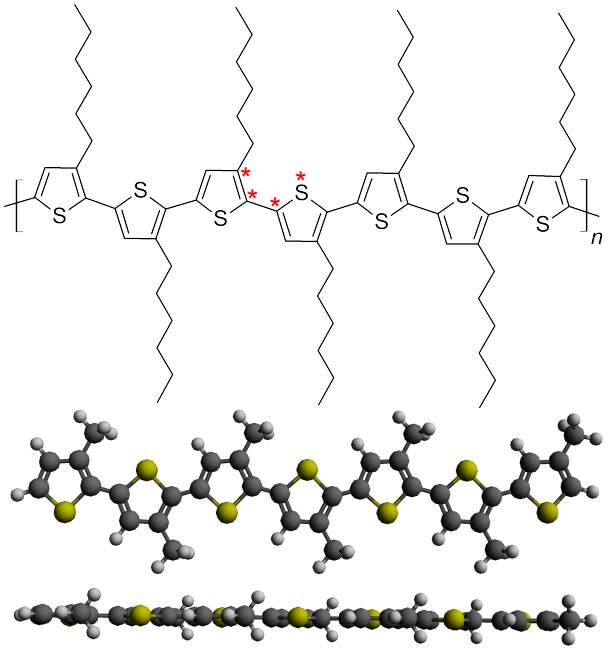

Figure 1: (Top) Chemical structure of regioregular P3HT. (Bottom) Two views of the optimized structure of the 3MT heptamer in the S_1 state, showing a C−C−C−S dihedral angle (red asterisks on P3HT structure) of 0°.

The photophysical and photochemical properties of P3HT have been studied with femtosecond laser spectroscopy to reveal exciton lifetime,[20] torsional relaxation,[21] exciton hopping,[22,23] self localization,[24,25] charge transfer,[26,27] charge generation,[3,28,29] and exciton dissociation of P3HT.[30,31] Excited-state polythiophenes in solution exhibit a near-infrared (NIR) absorption band centered at 1100 nm.[20,32] This induced absorption band, or an ESA band,[30,33] has been used to understand the relaxation dynamics of P3HT and charge transfer reaction with PCBM.[27,28] The NIR ESA band of P3HT films or aggregates has two components, that is, an exciton band at 1200 nm, which is a major component at early time, and a hole-polaron band at 1000 nm which is present several nanoseconds after charge separation.[20,27,34] Although there is vast literature on the ESA band of P3HT, a detailed understanding of the physical nature of this induced absorption band is still unavailable.

Recently, Ling et al. reported a computational study on the ESA of a different set of oligomers, namely, oligofluorenes, offering insight into the transitions that are involved.[35] These authors performed nonlinear-response time-dependent density functional theory (TD-DFT) calculations using the Coulomb-attenuated Becke 3-Parameter (Exchange), Lee, Yang, and Parr (CAM-B3LYP) functional on oligofluorenes ranging from the dimer to heptamer, showing that the NIR ESA band is due to a dominant $S_1 \rightarrow S_5$ transition. The CAM-B3LYP functional has been employed in other recent computational studies of conjugated oligomers, showing high-level performance in predicting the physical and chemical properties of these systems.[36–42] In this study, the electronic properties of the S_1 excited state of oligothiophenes are investigated using nonlinear-response TD-DFT. The computational methods used are shown in the Supporting Information (SI). The 3-hexylthiophene (3HT) oligomers are approximated using 3-methylthiophenes (3MT), as shown in Figure 1. We have performed calculations to show that substitution of the hexyl side-chains of oligothiophenes with methyl groups has negligible influences on its electronic structure, as shown in Figure S1 in SI. In addition, we have also shown that the use of the CAM-B3LYP functional is crucial in obtaining the ESA spectrum that agrees with experiment, as shown in Figure S2.

The optimized structure of the heptamer in the S_1 state is shown in Figure 1, highlighting the planar arrangement with a C−C−C−S (red asterisks) dihedral angle of 0°. The optimized structure in the S_0 state is given in Figure S3 of SI, showing that the ground-state geometry is nonplanar with an average dihedral angle of ∼30°. The structures of other oligomers are also shown in Figure S3, which agree with those by Bhatta et al. on 3HT oligomers.[43] In addition, Figure S4 shows that the length of the alkyl side-chains plays a negligible role in the optimized structure in the S_1 state. In a vertical excitation, an electronic transition occurs from the S_0 to the S_1* state, which exhibits the greatest Franck-Condon overlap with S_0. The subsequent relaxation from S_1* to S_1 induces planarization of the oligomers, which has been observed spectroscopically as a spectral shift in both ultrafast transient absorption and photoluminescence studies.[21,25] The torsional motions occur rapidly (∼100 fs), lowering the excited-state energy and increasing the effective conjugation length of the oligomers, which is evident in the changes of the C−C and C=C bond lengths in the S_0 and S_1 states. In the excited state, the shortening of the C−C and corresponding lengthening of the C=C bonds are characteristics of the aromatic-to-quinoid like transitions, indicating the presence of the exciton.[44] Interestingly, while the trimer displays a complete inversion to the quinoidal type geometry in the S_1 state, this distortion remains limited to the central region for larger oligomers, with a spatial extent of about three thiophene units. For the heptamer, however, the terminal thiophene rings in the S_1 state exhibit similar bond lengths to those in the S_0 state, suggesting that it can support localization of the exciton.[45,46]

Figure 2 shows the oscillator strengths of the ESA peaks of 3MT oligomers as a function of excitation energy. The ESA spectrum of the trimer has two contributions, that is, the $S_1 \rightarrow S_2$ and $S_1 \rightarrow S_3$ transitions with similar oscillator strengths. In contrast, the ESA spectra of the tetramer and pentamer have three different contributions, arising from the former transitions and $S_1 \rightarrow S_5$ transition. For the hexamer and heptamer, only the $S_1 \rightarrow S_2$ and $S_1 \rightarrow S_3$ transitions are the contributing transitions. The $S_1 \rightarrow S_3$ transition, however, has a substantially higher oscillator strength than the $S_1 \rightarrow S_2$ transition. Figure 2 also shows the significant increase in the oscillator strength of the $S_1 \rightarrow S_3$ transition as the oligomer lengthens, with it being the dominant transition for the heptamer. The effect of solvent on the ESA spectrum was also investigated and Figure S5 in SI shows the insignificant difference between the calculated ESA spectrum in tetrahydrofuran and vacuum.

The $S_1 \rightarrow S_3$ ESA peak position of the heptamer is close to the experimental value of P3HT, which is indicated by the dashed line

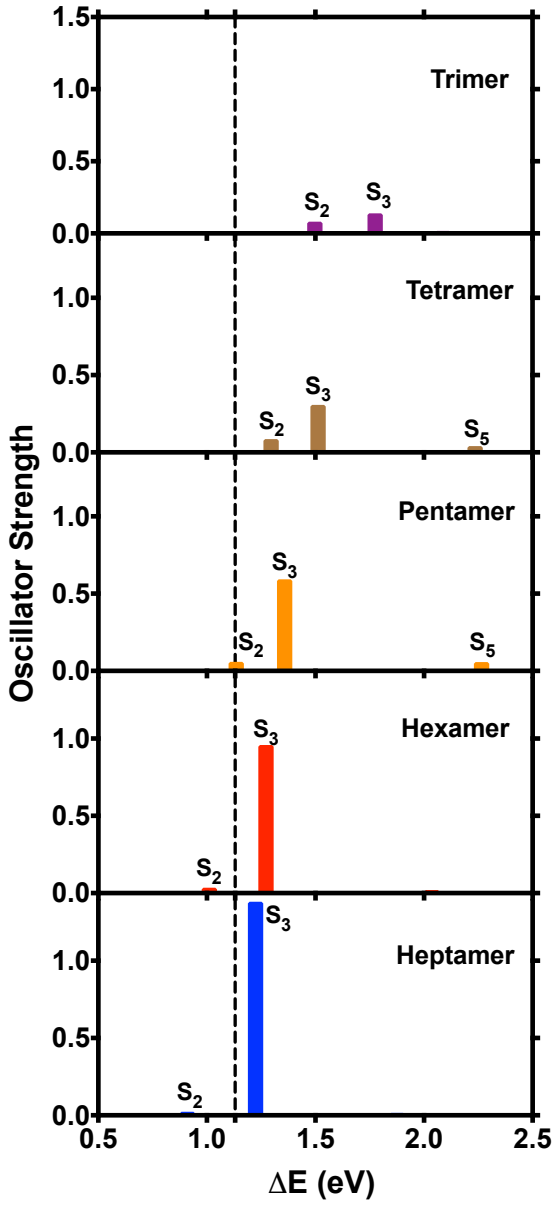

Figure 2: Calculated ESA peaks for 3MT oligomers. The excitation energies correspond to the transitions from the S_1 state to a higher-lying S_n excited state, where n ranges from 2 to 5. The vertical dashed line indicates the experimental ESA peak position of P3HT.[30]

in Figure 2. Furthermore, the $S_1 \rightarrow S_3$ energy gap of 3MT oligomers shows a red shift with oligomer length, as shown in SI (Figure S6), exhibiting a $1/n$ dependence, where n is the number of repeating units. This dependence has been observed for oligothiophenes[47–49] and suggests that only a minor decrease in the $S_1 \rightarrow S_3$ energy gap is expected for any oligomers longer than the heptamer. Therefore, the heptamer system is sufficiently large to yield quantitative results for comparison with experiment. In this case, the experimental ESA peak position of P3HT chains is 1.17 eV and the predicted value for the heptamer (1.22 eV) differs by only <0.1 eV, showing a good agreement.[30,32] This result is similar to a previous study by Ling et al., in which the predicted and experimental ESA peaks of polyfluorenes differ by <0.2 eV.[35] In order to demonstrate the agreement, Figure 3 shows the experimentally measured ESA spectrum of P3HT[30] and the calculated spectrum of the heptamer. The calculated spectrum was broadened using a Gaussian function with a best-fit full width at half maximum of 0.36 eV. The difference between the two spectral peaks in Figure 3 is 0.07 eV. In the inset of Figure 3, the calculated spectrum is shifted by this minor energy difference, showing an excellent agreement to the experimental spectrum.[30]

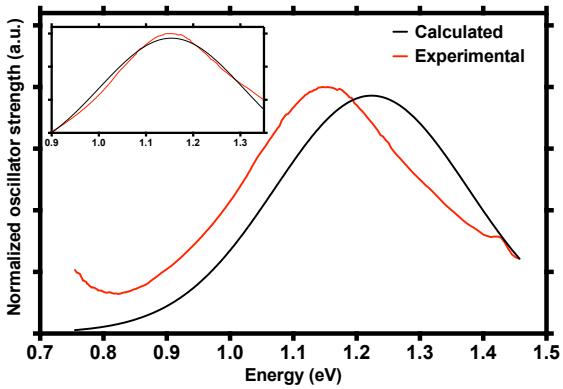

Figure 3: ESA spectra of P3HT from experiment (red),[30] and as calculated for the 3MT heptamer (black). The inset shows an excellent agreement between the spectra when the calculated spectrum is shifted by −0.07 eV.

The reproduction the ESA spectrum of P3HT using such a simplified system and relatively

nonresource intensive computational method is initially surprising, given that the accurate calculation of the ground-state absorption spectrum of conjugated polymers can be challenging.[39,50] In solution, thermal and solvent effects cause the polymer to adopt a random-coil geometry with a wide distribution of intermonomer angles and dihedrals. Consequently, the ground-state chromophores are highly disordered, and thus defining a chromophore precisely is a complex task.[51–53] Furthermore, the absorption spectrum is not solely due to any single chromophore but is composed of an ensemble of chromophores with a variety of environments and geometries. Choosing a representative selection of chromophores is a challenge, even before considering a suitable method and the associated computational costs. To address these obstacles, simulation of the optical properties of conjugated polymers is often performed using classical methods to obtain the polymer geometry and simplified quantum mechanical methods with the ability to scale to systems with hundreds or thousands of chromophores.[49,54,55] In contrast with the ground-state S_0 geometry, the excited S_1 state of P3HT is more ordered and well defined. As shown in Figure S3 and S4 in SI, the S_1 state adopts a planar geometry, regardless of the side-chain substituents. While the vertical $S_0 \rightarrow S_1{}^*$ excitation involves ∼20 thiophene units of a highly disordered chain, the exciton localizes to 5–10 monomeric units, driving the planarization of the chromophore site. Similar to the ground-state absorption, the ESA is also due to an ensemble of chromophores but in this case each individual chromophore can be sufficiently described as a planar oligothiophene of 5 to 10 monomeric units.

The excellent agreement between the measured ESA spectrum of P3HT and that of the 3MT heptamer calculated using TD-DFT with the CAM-B3LYP functional is consistent with a previous study.[35] Ling et al. showed that TD-DFT calculations using CAM-B3LYP produce ESA spectra that exhibit agreement with experiment,[35] demonstrating the importance of accounting for the long-range contributions to the electronic exchange interactions. In addition to excited-state properties, CAM-B3LYP includes charge-transfer contributions to electronic excitations. The application of CAM-B3LYP on predicting the charge-transfer properties of the excited states of a 3MT oligomer is discussed below. Additional results and further discussion on the choice of functional may be found in SI.

To reveal insight into the charge transfer character of the $S_1 \rightarrow S_3$ transition, we turn to the electron density change involved in this transition. The electron density difference, $\Delta\rho(r)$, between the excited state and ground state can be evaluated as

$$\Delta\rho(r) = \rho_{\text{excited}}(r) - \rho_{\text{ground}}(r) \qquad (1)$$

where $\rho_{\text{excited}}(r)$ and $\rho_{\text{ground}}(r)$ are the electron densities of the excited and ground states at position r. There is, however, no direct method to calculate the electron density changes of the $S_1 \rightarrow S_3$ transition. Therefore, eq 2 is used to relate the electron density changes of the $S_1 \rightarrow S_3$ transition to those of the $S_0 \rightarrow S_1$ and $S_0 \rightarrow S_3$ transitions.

$$\Delta\rho_{S_1\rightarrow S_3}(r) = \Delta\rho_{S_0\rightarrow S_3}(r) - \Delta\rho_{S_0\rightarrow S_1}(r) \qquad (2)$$

This approach provides an indirect route to obtaining the electron density change between the S_1 and S_3 states. On the basis of eq 1, an increase in electron density corresponds to more "electron" character, while a decrease in electron density corresponds to more "hole" character.

Figure 4 shows the electron density difference calculated for the $S_1 \rightarrow S_3$ transition of the heptamer. The increase in electron density is concentrated in the middle region of the oligomer, with the corresponding decrease occurring along the oligomer's ends, as indicated by the black arrows in Figure 4. The middle region of the 3MT heptamer undergoes a "switch" in the electron and hole positions in comparison with both the $S_0 \rightarrow S_1$ and $S_0 \rightarrow S_3$ transitions (SI, Figure S7). An increase in electron density occurs at the central sulfur atom for both the $S_0 \rightarrow S_1$ and $S_0 \rightarrow S_3$ transitions. For the $S_1 \rightarrow S_3$ transition, however, the same sul-

fur atom shows an electron density decrease, indicating charge movement, or intramolecular charge transfer, along the backbone of the oligomer. This "switch" has also been observed by Denis et al. for the $S_1 \rightarrow S_n$ transition compared with the $S_0 \rightarrow S_1$ transition for fluorene homopolymers and fluorene-based copolymers.[56] The electron density difference for the $S_1 \rightarrow S_3$ transition of other oligomers exhibits a similar behavior and is shown in Figure S8 in SI. The intramolecular charge transfer characters were also investigated using a natural transition orbital analysis and the results are shown in SI (Figure S9).

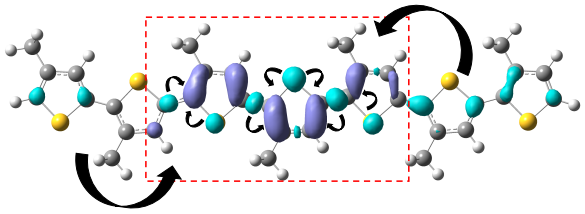

Figure 4: Electron density difference of the 3MT heptamer for the $S_1 \rightarrow S_3$ transition, where the violet and turquoise regions represent the increase and decrease, respectively, in electron density. The arrows serve to highlight the movement of charge. The isosurface value used to visualize the electron density difference is 0.0005 $Å^{-3}$

The intramolecular charge transfer process is a primary indicator of the capacity for an exciton to dissociate into free charge carriers. Experimentally, we have used transient absorption spectroscopy to demonstrate charge carrier generation in P3HT chains through targeted photoexcitation of the ESA band.[30] We have used a femtosecond pump-push-probe technique to isolate the relaxation processes and products of the higher-lying S_n state. The computational work presented here offers new insight, confirming that charge carrier generation occurs on isolated polymer chains through an intramolecular charge-transfer intermediate. In the experiment, the visible pump-pulse vertically excites P3HT from the ground-state to form the S_1^* singlet exciton. The high-energy exciton then undergoes relaxation within ∼100 fs to the S_1 state. The NIR push-pulse is tuned to match the ESA band, further exciting the S_1 exciton to a high-energy state, S_n. From the results in this study (Figure 2), we can now assign the previously unknown S_n state to S_3. From the S_3 state the exciton rapidly relaxes back to S_1, but in the experiment ∼11% of the S_3 exciton population directly returns to the ground-state rather than back through S_1. This phenomenon was attributed to dissociation of the exciton into electron and hole-polaron charge carriers. We have now shown that such dissociation on isolated chains is possible due to the charge transfer nature of the S_3 state, where the movement of electrons occurs predominantly from the outer regions to the center of the chromophore. Because the separated electrons and holes are still spatially restricted to a single P3HT chain, geminate recombination occurs rapidly, resulting in a direct return to the S_0 ground-state.

In short, we have used nonlinear response TD-DFT to gain insight into the ESA band of P3HT in the NIR region. Computational studies using the CAM-B3LYP functional have been conducted on the 3MT oligomers ranging from the trimer to heptamer to show that the ESA band corresponds to the $S_1 \rightarrow S_3$ transition. The oscillator strength of this transition increases as a function of oligomer length and it becomes the dominant transition of the 3MT heptamer. The predicted energy of the $S_1 \rightarrow S_3$ transition exhibits an excellent agreement with experiment. The results also reveal the charge transfer character of the $S_1 \rightarrow S_3$ transition, which is consistent with experimental results on exciton dissociation because of optical pumping of the singlet exciton.

Acknowledgement This research was undertaken with the assistance of resources provided at the Phoenix High Performance Computing service at the University of Adelaide. We acknowledge the assistance of Mr. Rohan J. Hudson in the DFT calculations and Dr. David M. Huang for his comments and suggestions for this manuscript.

Supporting Information Available

(1) Computational methods, (2) influence of side-chain substituents, functional, and solvation on computed excited state transitions, (3) geometry of 3HT and 3MT trimers, 3MT tetramer to heptamer optimized in S_0 and S_1 states, (4) calculated $S_1 \rightarrow S_3$ transition energies with 3MT oligomer length, (5) electron density difference of 3MT heptamer for $S_0 \rightarrow S_1$ and $S_0 \rightarrow S_3$ transitions, and $S_1 \rightarrow S_3$ transitions for 3MT trimer to hexamer, (6) natural transition orbitals of the $S_0 \rightarrow S_1$ and $S_0 \rightarrow S_3$ transitions of the 3MT heptamer, (7) input commands to compute excited state absorptions using Dalton2016 software, (8) Cartesian coordinates for all molecular structures.

References

(1) Halls, J. J. M.; Walsh, C. A.; Greenham, N.; Marseglia, E. A.; Friend, R.; Moratti, S. C.; Holmes, A. Efficient Photodiodes from Interpenetrating Polymer Networks. *Nature* **1995**, *376*, 498–500.

(2) Yu, G.; Gao, J.; Hummelen, J. C.; Wudl, F.; Heeger, A. J. Polymer Photovoltaic Cells: Enhanced Efficiencies via a Network of Internal Donor-Acceptor Heterojunctions. *Science* **1995**, *270*, 1789–1791.

(3) Clarke, T. M.; Durrant, J. R. Charge Photogeneration in Organic Solar Cells. *Chem. Rev.* **2010**, *110*, 6736–6767.

(4) Brédas, J.-L.; Norton, J. E.; Cornil, J.; Coropceanu, V. Molecular Understanding of Organic Solar Cells: The Challenges. *Acc. Chem. Res.* **2009**, *42*, 1691–1699, PMID: 19653630.

(5) Blom, P.; Mihailetchi, V.; Koster, L.; Markov, D. Device Physics of Polymer:fullerene Bulk Heterojunction Solar Cells. *Adv. Mater.* **2007**, *19*, 1551–1566.

(6) Caruso, D.; Troisi, A. Long-range Exciton Dissociation in Organic Solar Cells. *Proc. Natl. Acad. Sci. U.S.A.* **2012**, *109*, 13498–13502.

(7) Bakulin, A. A.; Rao, A.; Pavelyev, V. G.; van Loosdrecht, P. H. M.; Pshenichnikov, M. S.; Niedzialek, D.; Cornil, J.; Beljonne, D.; Friend, R. H. The Role of Driving Energy and Delocalized States for Charge Separation in Organic Semiconductors. *Science* **2012**, *335*, 1340–1344.

(8) Gélinas, S.; Rao, A.; Kumar, A.; Smith, S. L.; Chin, A. W.; Clark, J.; van der Poll, T. S.; Bazan, G. C.; Friend, R. H. Ultrafast Long-Range Charge Separation in Organic Semiconductor Photovoltaic Diodes. *Science* **2014**, *343*, 512.

(9) Hotta, S.; Soga, M.; Sonoda, N. Novel Organosynthetic Routes to Polythiophene and its Derivatives. *Synth. Met.* **1988**, *26*, 267–279.

(10) Dang, M. T.; Hirsch, L.; Wantz, G.; Wuest, J. D. Controlling the Morphology and Performance of Bulk Heterojunctions in Solar Cells. Lessons Learned from the Benchmark Poly(3-hexylthiophene):[6,6]-Phenyl-C61-butyric Acid Methyl Ester System. *Chem. Rev.* **2013**, *113*, 3734–3765.

(11) Mehmood, U.; Al-Ahmed, A.; Hussein, I. A. Review on Recent Advances in Polythiophene Based Photovoltaic Devices. *Renewable Sustainable Energy Rev.* **2016**, *57*, 550–561.

(12) Dang, M. T.; Hirsch, L.; Wantz, G. P3HT:PCBM, Best Seller in Polymer Photovoltaic Research. *Adv. Mater.* **2011**, *23*, 3597–3602.

(13) Samitsu, S.; Shimomura, T.; Heike, S.; Hashizume, T.; Ito, K. Effective Production of Poly(3-alkylthiophene) Nanofibers by means of Whisker Method using Anisole Solvent: Structural, Optical,

and Electrical Properties. *Macromolecules* **2008**, *41*, 8000–8010.

(14) Sun, S.; Salim, T.; Wong, L. H.; Foo, Y. L.; Boey, F.; Lam, Y. M. A New Insight into Controlling Poly(3-hexylthiophene) Nanofiber Growth Through a Mixed-solvent Approach for Organic Photovoltaics Applications. *J. Mater. Chem.* **2011**, *21*, 377–386.

(15) Ma, W.; Yang, C.; Gong, X.; Lee, K.; Heeger, A. Thermally Stable, Efficient Polymer Solar Cells with Nanoscale Control of the Interpenetrating Network Morphology. *Adv. Funct. Mater.* **2005**, *15*, 1617–1622.

(16) Vanlaeke, P.; Swinnen, A.; Haeldermans, I.; Vanhoyland, G.; Aernouts, T.; Cheyns, D.; Deibel, C.; DaHaen, J.; Heremans, P.; Poortmans, J. et al. P3HT/PCBM Bulk Heterojunction Solar Cells: Relation between Morphology and Electro-optical Characteristics. *Sol. Energy Mater. Sol. Cells* **2006**, *90*, 2150–2158.

(17) Kim, Y.; Cook, S.; Tuladhar, S. M.; Choulis, S. A.; Nelson, J.; Durrant, J. R.; Bradley, D. D. C.; Giles, M.; McCulloch, I.; Ha, C.-S. et al. A Strong Regioregularity Effect in Self-organizing Conjugated Polymer Films and High-efficiency Polythiophene:Fullerene Solar Cells. *Nat. Mater.* **2006**, *5*, 197–203.

(18) Marsh, R. A.; Hodgkiss, J. M.; Albert-Seifried, S.; Friend, R. H. Effect of Annealing on P3HT:PCBM Charge Transfer and Nanoscale Morphology Probed by Ultrafast Spectroscopy. *Nano Lett.* **2010**, *10*, 923–930.

(19) Laquai, F.; Andrienko, D.; Mauer, R.; Blom, P. W. M. Charge Carrier Transport and Photogeneration in P3HT:PCBM Photovoltaic Blends. *Macromol. Rapid Commun.* **2015**, *36*, 1001–1025.

(20) Cook, S.; Furube, A.; Katoh, R. Analysis of the Excited States of Regioregular Polythiophene P3HT. *Energy Environ. Sci.* **2008**, *1*, 294–299.

(21) Parkinson, P.; Muller, C.; Stingelin, N.; Johnston, M. B.; Herz, L. M. Role of Ultrafast Torsional Relaxation in the Emission from Polythiophene Aggregates. *J. Phys. Chem. Lett.* **2010**, *1*, 2788–2792.

(22) Wells, N. P.; Boudouris, B. W.; Hillmyer, M. A.; Blank, D. A. Intramolecular Exciton Relaxation and Migration Dynamics in Poly(3-hexylthiophene). *J. Phys. Chem. C* **2007**, *111*, 15404–15414.

(23) Wells, N. P.; Blank, D. A. Correlated Exciton Relaxation in Poly(3-hexylthiophene). *Phys. Rev. Lett.* **2008**, *100*, 086403.

(24) Banerji, N.; Cowan, S.; Vauthey, E.; Heeger, A. J. Ultrafast Relaxation of the Poly(3-hexylthiophene) Emission Spectrum. *J. Phys. Chem. C* **2011**, *115*, 9726–9739.

(25) Busby, E.; Carroll, E. C.; Chinn, E. M.; Chang, L.; Moulé, A. J., A. J.e; Larsen, D. S. Excited-State Self-trapping and Ground-state Relaxation Dynamics in Poly(3-hexylthiophene) Resolved with Broadband Pump-dump-probe Spectroscopy. *J. Phys. Chem. Lett.* **2011**, *2*, 2764–2769.

(26) Song, Y.; Clafton, S. N.; Pensack, R. D.; Kee, T. W.; Scholes, G. D. Vibrational Coherence Probes the Mechanism of Ultrafast Electron Transfer in Polymer–fullerene Blends. *Nat. Commun.* **2014**, *5*, 4933.

(27) Clafton, S. N.; Huang, D. M.; Massey, W. R.; Kee, T. W. Femtosecond Dynamics of Excitons and Hole-polarons in Composite P3HT/PCBM Nanoparticles. *J. Phys. Chem. B* **2013**, *117*, 4626–4633.

(28) Guo, J.; Ohkita, H.; Benten, H.; Ito, S. Charge Generation and Recombination Dynamics in Poly(3-hexylthiophene)/fullerene Blend Films with Different Regioregularities and Morphologies. *J. Am. Chem. Soc.* **2010**, *132*, 6154–6164.

(29) Chen, K.; Barker, A. J.; Reish, M. E.; Gordon, K. C.; Hodgkiss, J. M. Broadband Ultrafast Photoluminescence Spectroscopy Resolves Charge Photogeneration via Delocalized Hot Excitons in Polymer:Fullerene Photovoltaic Blends. *J. Am. Chem. Soc.* **2013**, *135*, 18502–18512.

(30) Tapping, P. C.; Kee, T. W. Optical Pumping of Poly(3-hexylthiophene) Singlet Excitons Induces Charge Carrier Generation. *J. Phys. Chem. Lett.* **2014**, *5*, 1040–1047.

(31) Kee, T. W. Femtosecond Pump-Push-Probe and Pump-Dump-Probe Spectroscopy of Conjugated Polymers: New Insight and Opportunities. *J. Phys. Chem. Lett.* **2014**, *5*, 3231–3240.

(32) Kraabel, B.; Moses, D.; Heeger, A. J. Direct Observation of the Intersystem Crossing in Poly(3-octylthiophene). *J. Chem. Phys.* **1995**, *103*, 5102–5108.

(33) Yu, W.; Magnanelli, T. J.; Zhou, J.; Bragg, A. E. Structural Heterogeneity in the Localized Excited States of Poly(3-hexylthiophene). *J. Phys. Chem. B* **2016**, *120*, 5093–5102.

(34) Guo, J.; Ohkita, H.; Benten, H.; Ito, S. Near-IR Femtosecond Transient Absorption Spectroscopy of Ultrafast Polaron and Triplet Exciton Formation in Polythiophene Films with Different Regioregularities. *J. Am. Chem. Soc.* **2009**, *131*, 16869–16880.

(35) Ling, S.; Schumacher, S.; Galbraith, I.; Paterson, M. J. Excited-State Absorption of Conjugated Polymers in the Near-Infrared and Visible: A Computational Study of Oligofluorenes. *J. Phys. Chem. C* **2013**, *117*, 6889–6895.

(36) Borges, I.; Uhl, E.; Modesto-Costa, L.; Aquino, A. J. A.; Lischka, H. Insight into the Excited State Electronic and Structural Properties of the Organic Photovoltaic Donor Polymer Poly(thieno[3,4-b]thiophene benzodithiophene) by Means of ab Initio and Density Functional Theory. *J. Phys. Chem. C* **2016**, *120*, 21818–21826.

(37) Oliveira, E. F.; Roldao, J. C.; Milin-Medina, B.; Lavarda, F. C.; Gierschner, J. Calculation of Low Bandgap Homopolymers: Comparison of TD-DFT Methods with Experimental Oligomer Series. *Chem. Phys. Lett.* **2016**, *645*, 169–173.

(38) Van den Brande, N.; Van Lier, G.; Da Pieve, F.; Van Assche, G.; Van Mele, B.; De Proft, F.; Geerlings, P. A Time Dependent DFT Study of the Efficiency of Polymers for Organic Photovoltaics at the Interface with PCBM. *RSC Adv.* **2014**, *4*, 52658–52667.

(39) McCormick, T. M.; Bridges, C. R.; Carrera, E. I.; DiCarmine, P. M.; Gibson, G. L.; Hollinger, J.; Kozycz, L. M.; Seferos, D. S. Conjugated Polymers: Evaluating DFT Methods for More Accurate Orbital Energy Modeling. *Macromolecules* **2013**, *46*, 3879–3886.

(40) Reish, M. E.; Nam, S.; Lee, W.; Woo, H. Y.; Gordon, K. C. A Spectroscopic and DFT Study of the Electronic Properties of Carbazole-Based DA Type Copolymers. *J. Phys. Chem. C* **2012**, *116*, 21255–21266.

(41) Limacher, P. A.; Mikkelsen, K. V.; Lthi, H. P. On the Accurate Calculation of Polarizabilities and Second Hyperpolarizabilities of Polyacetylene Oligomer Chains using the CAM-B3LYP Density Functional. *J. Chem. Phys.* **2009**, *130*, 194114.

(42) Zhang, S.; Qu, Z.; Tao, P.; Brooks, B.; Shao, Y.; Chen, X.; Liu, C. Quantum Chemical Study of the Ground

and Excited State Electronic Structures of Carbazole Oligomers with and without Triarylborane Substitutes. *J. Phys. Chem. C* **2012**, *116*, 12434–12442, PMID: 22754601.

(43) Bhatta, R. S.; Yimer, Y. Y.; Tsige, M.; Perry, D. S. Conformations and Torsional Potentials of Poly(3-hexylthiophene) Oligomers: Density Functional Calculations Up to the Dodecamer. *Comput. Theor. Chem.* **2012**, *995*, 36–42.

(44) Tsoi, W. C.; James, D. T.; Kim, J. S.; Nicholson, P. G.; Murphy, C. E.; Bradley, D. D. C.; Nelson, J.; Kim, J.-S. The Nature of In-Plane Skeleton Raman Modes of P3HT and Their Correlation to the Degree of Molecular Order in P3HT:PCBM Blend Thin Films. *J. Am. Chem. Soc.* **2011**, *133*, 9834–9843.

(45) Gierschner, J.; Cornil, J.; Egelhaaf, H.-J. Optical Bandgaps of π-Conjugated Organic Materials at the Polymer Limit: Experiment and Theory. *Adv. Mater.* **2007**, *19*, 173–191.

(46) Barford, W.; Lidzey, D. G.; Makhov, D. V.; Meijer, A. J. H. Exciton Localization in Disordered Poly(3-hexylthiophene). *J. Chem. Phys.* **2010**, *133*, 044504.

(47) Bidan, G.; De Nicola, A.; Enée, V.; Guillerez, S. Synthesis and UV–visible Properties of Soluble Regioregular Oligo(3-octylthiophenes), Monomer to Hexamer. *Chem. Mater.* **1998**, *10*, 1052–1058.

(48) Zhao, M.; Singh, B. P.; Prasad, P. N. A Systematic Study of Polarizability and Microscopic Thirdorder Optical Nonlinearity in Thiophene Oligomers. *J. Chem. Phys.* **1988**, *89*, 5535–5541.

(49) Tapping, P. C.; Clafton, S. N.; Schwarz, K. N.; Kee, T. W.; Huang, D. M. Molecular-Level Details of Morphology-Dependent Exciton Migration in Poly(3-hexylthiophene) Nanostructures. *J. Phys. Chem. C* **2015**, *119*, 7047–7059.

(50) Böckmann, M.; Doltsinis, N. L. Can Excited Electronic States of Macromolecules with Extended Pi-systems be Reliably Predicted? A Case Study on P3HT. *Front. Mater.* **2015**, *2*, 25.

(51) Beenken, W. J. D.; Pullerits, T. Spectroscopic Units in Conjugated Polymers: A Quantum Chemically Founded Concept? *J. Phys. Chem. B* **2004**, *108*, 6164–6169.

(52) Barford, W.; Marcus, M. Theory of Optical Transitions in Conjugated Polymers. I. Ideal Systems. *J. Chem. Phys.* **2014**, *141*, 164101.

(53) Marcus, M.; Tozer, O. R.; Barford, W. Theory of Optical Transitions in Conjugated Polymers. II. Real Systems. *J. Chem. Phys.* **2014**, *141*, 164102.

(54) Ma, H.; Qin, T.; Troisi, A. Electronic Excited States in Amorphous MEH-PPV Polymers from Large-Scale First Principles Calculations. *J. Chem. Theory Comput.* **2014**, *10*, 1272–1282.

(55) Wang, L.; Beljonne, D. Optical Properties of Regioregular Poly(3-hexylthiophene) Aggregates from Fully Atomistic Investigations. *CrystEngComm* **2016**, *18*, 7297–7304.

(56) Denis, J.-C.; Ruseckas, A.; Hedley, G. J.; Matheson, A. B.; Paterson, M. J.; Turnbull, G. A.; Samuel, I. D. W.; Galbraith, I. Self-trapping and Excited State Absorption in Fluorene Homo-polymer and Copolymers with Benzothiadiazole and Tri-phenylamine. *Phys. Chem. Chem. Phys.* **2016**, *18*, 21937–21948.

Origin of the Excited-State Absorption Spectrum of Polythiophene (Supporting Information)

Ras Baizureen Roseli, Patrick C. Tapping, and Tak W. Kee*

Department of Chemistry, The University of Adelaide, South Australia 5005, Australia

E-mail: tak.kee@adelaide.edu.au

Phone: +61-8-8313-5039

Computational Methods

Computational calculations were performed for a set of regioregular 3MT oligomers from the trimer up to heptamer using the Gaussian 09 and Dalton2016 packages.[1,2] In all calculations, the hexyl side chains were replaced by methyl groups. The molecular structures of the ground-state geometries were optimized with the CAM-B3LYP exchange-correlation functional with the 6-31(d,p) basis set using the Gaussian 09 package. Ground-state geometries were optimized without imposing any symmetry constraints. All other calculations involving the excited states were based on the time-dependent DFT/CAM-B3LYP method with the same basis set using both the Gaussian 09 package and Dalton2016 packages.[1,2] The excitation energies (absorption) were obtained using the linear response approach and optimization was performed using Gaussian 09 to obtain the optically active lowest excited S_1 state geometry. Calculations were also performed using the B3LYP functional to study the effects of functional on the calculation results.

The optimized geometry of the S_1 state was used to calculate the first-order transition moments between S_1 and higher lying excited states (keyword DOUBLE RESIDUE), which are based on the quadratic response function calculations (keyword QUADRA) using the Dalton2016 package. For the first-order transition moments calculations, each component of the one-photon transition matrix element was calculated within a limited number of the excited states. The lowest 5 excited states (keyword ROOT) were taken into account for all oligomers. The input parameters used to perform the calculations using the Dalton2016 package are available below. The calculated excitation energies and transition dipoles were used to calculate the oscillator strength for the electronic transitions from the S_1 to higher lying excited states S_n where n ranges from 2 to 5. All calculations were conducted in vacuum to reduce computational time.

The calculations on the effect of solvent were performed using the polarized continuum model, as implemented in Gaussian 09 and Dalton2016 packages. The characteristics of the electronic transition was investigated using natural transition orbitals (NTOs).[3] The electron density difference between the ground and excited state was calculated using Multiwfn, which is a program for wavefunction analysis.[4] The electron density difference between the lowest-lying excited state, S_1, and higher lying excited state, S_n, was calculated using the cubman utilities within the Gaussian 09 package.[1] The visualization of the NTOs and electron density difference was undertaken using the Avogadro software package and GaussView, respectively.[5,6]

Effect of Side-Chain on the ESA Band

First, we present the results of replacing the hexyl side chains of 3HT oligomers with methyl groups. According to previous studies, the alkyl side-chains have negligible influence on the electronic structure and optical properties of conjugated polymers.[7] To demonstrate this is also valid for P3HT, calculations were performed for the 3HT and 3MT trimers, with hexyl and methyl side chains, respectively, to study the effect of side chain on the excited-state absorption band. The excited-state absorption peaks of the 3HT and 3MT trimers are presented in Figure S1, which show that there is significant overlap in the energies for the $S_1 \rightarrow S_2$ and $S_1 \rightarrow S_3$ transitions for both oligomers. Furthermore, there is also an overlap for the $S_1 \rightarrow S_5$ transition but the calculated band for 3HT is insufficiently intense to appear in Figure S1. In contrast, for the $S_1 \rightarrow S_4$ transition the energies for 3HT and 3MT differ by 0.2 eV. This discrepancy is expected to have an insignificant effect because this transition has a low oscillator strength. Overall, there is a less than 1% difference in oscillator strength and the energy of the electronic states involved in the

excited-state absorption band between using the methyl group and the hexyl side-chains. As a result of this minor difference, the hexyl side-chains of the thiophene oligomers are replaced with methyl groups in this study, which is expected to maintain the accuracy of the results.

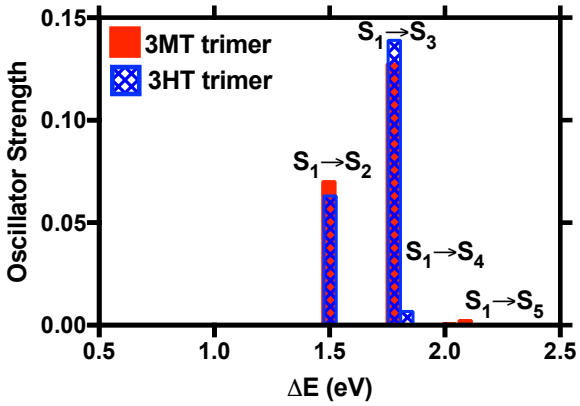

Figure S1: Computed excited state absorption (ESA) peaks of 3-hexylthiophene (3HT) trimer compared to 3-methylthiophene (3MT) trimer using CAM-B3LYP.

Effect of Functional on the ESA Band

Next, selecting a functional that best describes the expected behaviors of a system is an important factor in formulating density functional theory calculations. The B3LYP functional has been widely used in previous DFT studies of the properties of oligothiophene derivatives.[8,9] While no DFT studies on the excited-state absorption spectra of oligothiophenes have been reported, there is only one report that demonstrates the use of time-dependent density functional theory to calculate the excited-state absorption spectra of fluorene oligomers.[10] The study conducted by Ling et al. shows that the use of CAM-B3LYP functional provides an excellent agreement with experiment.[10] In addition to calculations of the excited states, the CAM-B3LYP functional has been shown to perform well for describing ground-state properties of conjugated polymer systems.[11]

In order to study the effects of the different functionals, calculations have been performed using the B3LYP and CAM-B3LYP functionals. Figure S2 shows that the excited-state absorption peaks of the 3MT trimer and pentamer with B3LYP (blue) and CAM-B3LYP (red) functionals as a function of energy (ΔE). First, CAM-B3LYP predicts that the $S_1 \rightarrow S_3$ is the major transition, whereas the calculation results using B3LYP show that $S_1 \rightarrow S_2$ is the main transition. Second, although the energy of the $S_1 \rightarrow S_2$ transition for the 3MT trimer calculated using B3LYP is close to the experimentally measured excited-state absorption peak position, the energy of the same transition for the pentamer shows a substantial red-shift, deviating from the experimentally measured value. It is likely that the $S_1 \rightarrow S_2$ transition will undergo further red-shift in energy as the oligomer length increases. It is expected that the excited-state absorption peaks predicted using the B3LYP functional will deviate more than 65% from the experimental value at an oligomer length of 7 units, which is the expected chromophore length as shown by several studies.[12–14] In contrast, the excited-state absorption ($S_1 \rightarrow S_3$) predicted by CAM-B3LYP approaches the experimentally measured value as shown in Figure S2 and is discussed below. As a consequence, we argue that the B3LYP functional is incapable of predicting the excited-state absorption spectrum of the 3MT oligomers accurately. The results show that the use of the CAM-B3LYP functional is crucial

in obtaining the excited-state absorption spectrum that agrees with experiment. CAM-B3LYP combines the hybrid functional B3LYP and a long-range correction in electronic exchange interactions.[15] It is a range-separated hybrid functional with 19% Hartree-Fock exchange at short range but with 65% HF exchange at long range.[15] CAM-B3LYP has been used to study the nonlinear optical properties of small molecular systems and its accuracy rivals those of much more resource-intensive methods including coupled cluster theory.[16] Alternate long-range corrected functionals such as the more-recently developed ωB97X-D are likely also suitable for this application.[17,18] While the Dalton2016 software package used to compute the excited-state absorptions does not natively implement ωB97X, we do not expect the results to differ dramatically from those produced by CAM-B3LYP.

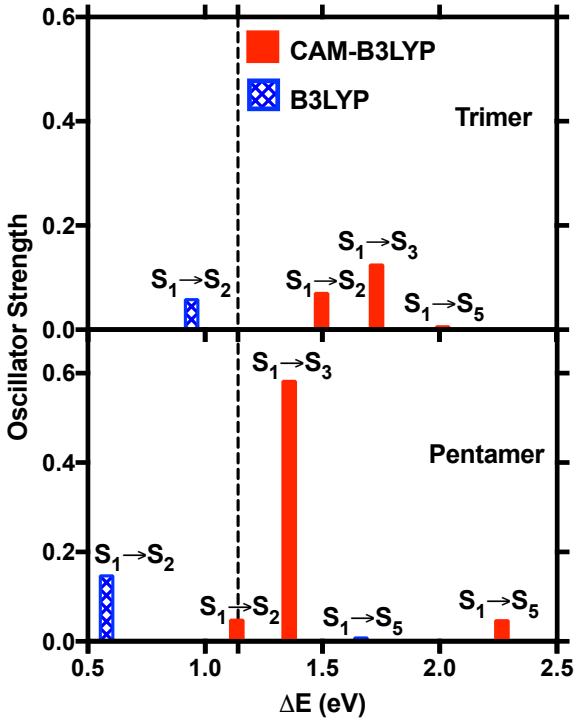

Figure S2: Calculated excitation energy of the $S_1 \rightarrow S_n$ transitions for 3MT trimer and pentamer using B3LYP (checkered blue) and CAM-B3LYP (solid red) functionals. The vertical dashed line indicates the experimental ESA energy of P3HT.[19]

Molecular Structures

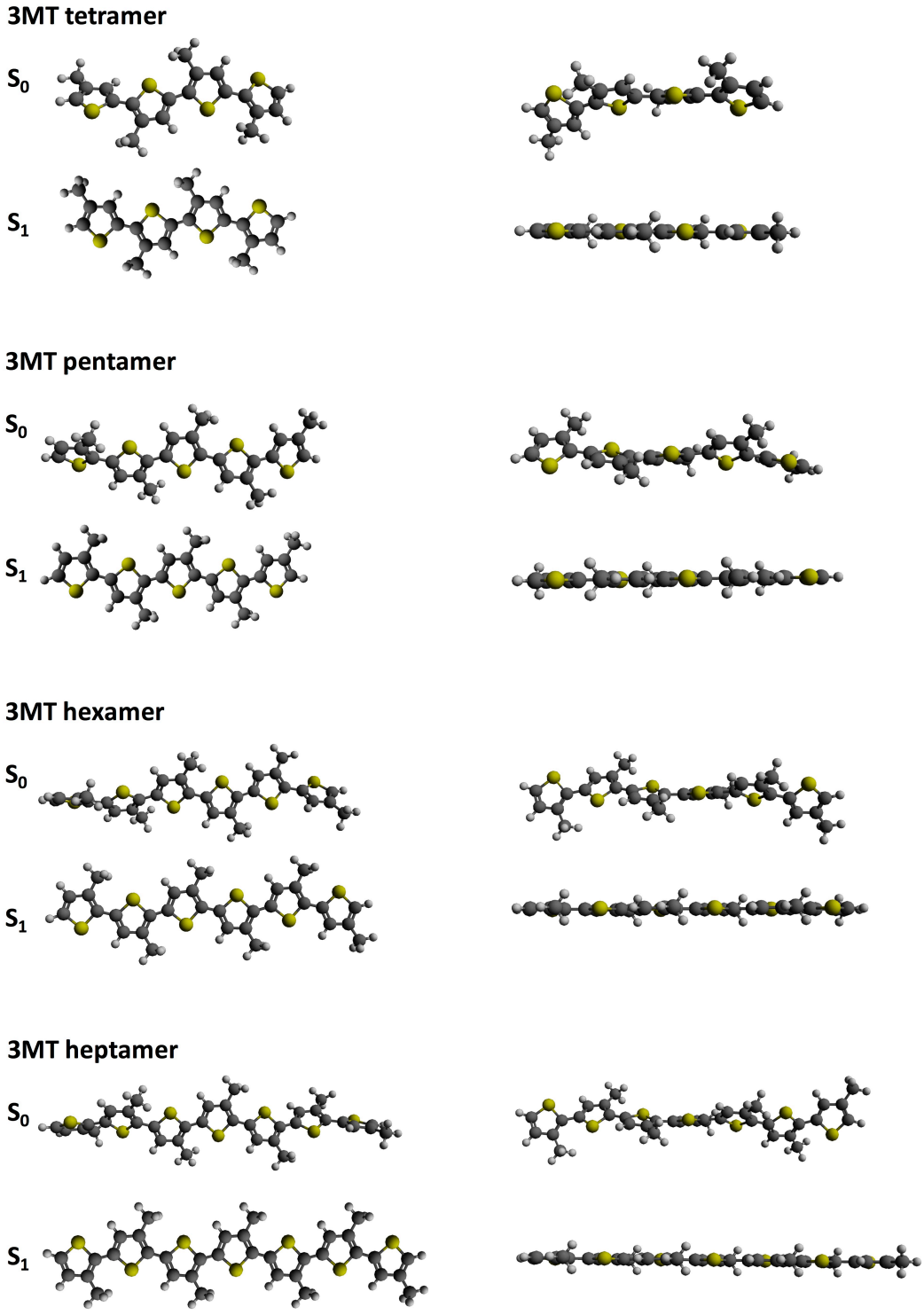

Figure S3: Optimized geometries of 3MT oligomers at S_0 and S_1 states from side (left) and top (right) views. Sulphur, carbon or hydrogen atoms are represented by yellow, grey or white spheres, respectively.

As the hexyl side-chains of the thiophene oligomers are replaced with methyl groups, calculations to study the effect of side-chains on the dihedral angles in the S_0 and S_1 states were performed on both the 3HT and 3MT trimers. The results show that the C−C−C−S dihedral angle of the 3HT trimer is 45.2° in the S_0 state, while the 3MT trimer dihedral is 31.6°, as shown in Figure S4. Although the dihedral angles of the two species are different in the S_0 state, the S_1 state of both species planarize to a dihedral angle of 0° (Figure S4). The difference in the dihedral angles in the S_0 state is expected to have a negligible effect on the calculated excited-state absorption bands of the thiophene oligomers. This is because the relevant excited-state absorption bands that are observed experimentally originate from the S_1 state, not the S_1^* state produced as a result of a vertical transition. As we have already noted, the rapid relaxation of S_1^* to S_1, on the order of ∼100 fs, is primarily through the planarization of the chromophore.[20–22]

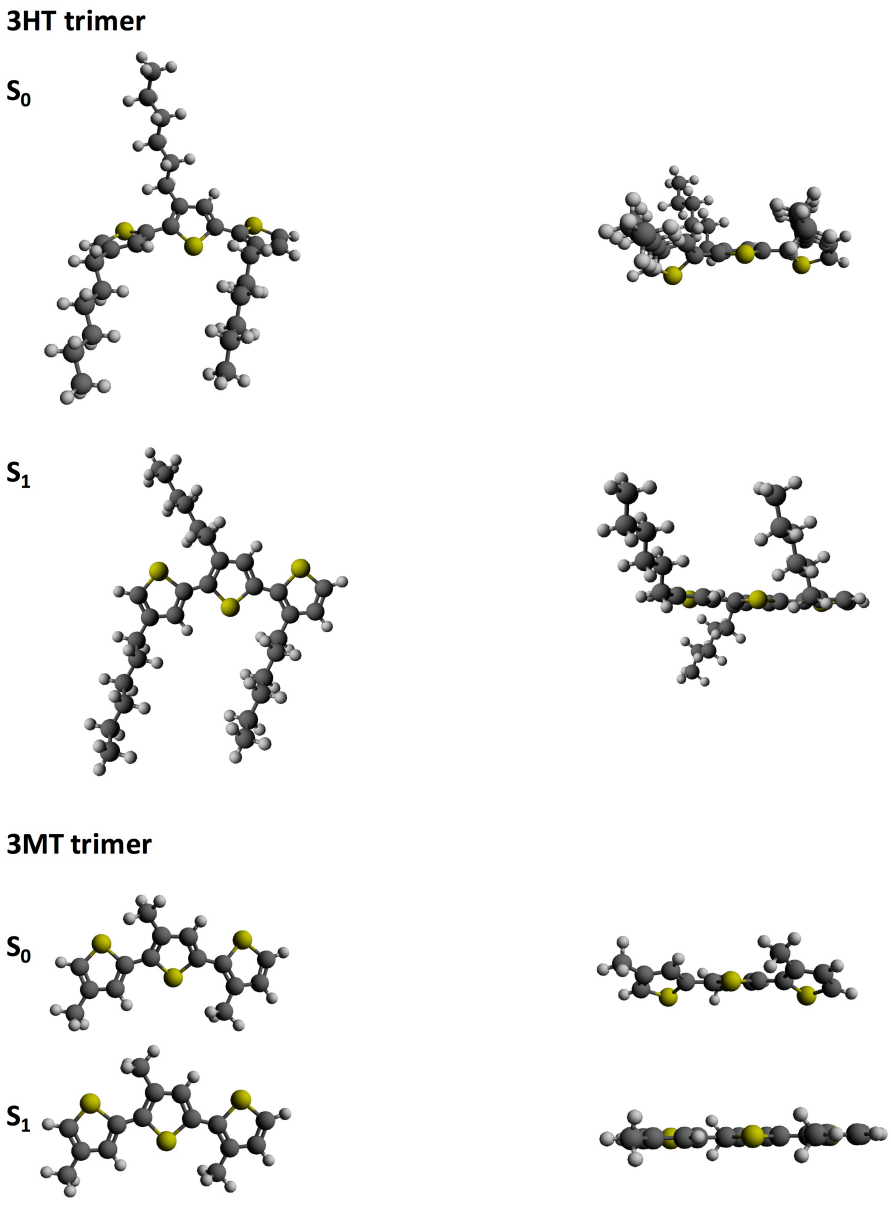

Figure S4: Optimized geometries of 3HT and 3MT trimer at S_0 and S_1 states from side (left) and top (right) views. Sulphur, carbon or hydrogen atoms are represented by yellow, grey or white spheres, respectively.

Effect of Solvation on the ESA Band

In order to calculate the excited-state absorption spectrum of the thiophene oligomers, we address the effect of solvent in the calculation results. The relevant experimental measurements were conducted in organic solvents including tetrahydrofuran (THF),[19] xylene,[23] chloroform and chlorobenzene.[21,24,25] In this case, we choose THF and the 3MT trimer as a representative model system for investigations on the effect of solvent in the excited-state absorption peaks of 3MT oligomers. Figure S5 shows the predicted excited-state absorption peaks of the 3MT trimer in THF in comparison to vacuum. First, the calculated excited-state absorption peaks of the 3MT trimer in vacuum and THF both show a major component due to the $S_1 \rightarrow S_3$ transition. Second, the energy of the $S_1 \rightarrow S_3$ transition for the 3MT trimer calculated in THF and in vacuum shows an insignificant difference of 0.1 eV. Furthermore, the energy differences for the $S_1 \rightarrow S_2$ and $S_1 \rightarrow S_5$ transitions for the 3MT trimer calculated in THF and in vacuum follow a similar trend, indicating that the inclusion of THF in the calculations increases the energy for all of the peaks by at most 0.1 eV, corresponding to change of less than 6%. These results agree with the study conducted by Denis et al., which shows that the calculated excited-state absorption energy of the fluorene pentamer in solvent and in vacuum only differ by 0.07 eV, corresponding to a change of less than 5%.[26] These authors concluded that the effect of solvent is minor and inclusion of solvent leads to similar results as those from calculations performed in vacuum. Furthermore, a previous study on conjugated polymers by Salzner showed that the effect of solvent appears to diminish as the system size increases.[27] This phenomenon suggests that the inclusion of solvent has a minor effect on the results as the oligomer length increases. As a consequence, all the calculations performed in this study were on 3MT oligomers in vacuum, which is identical to the approach taken by Ling et al. for the calculations on the excited-state absorption spectrum of fluorene oligomers.[10]

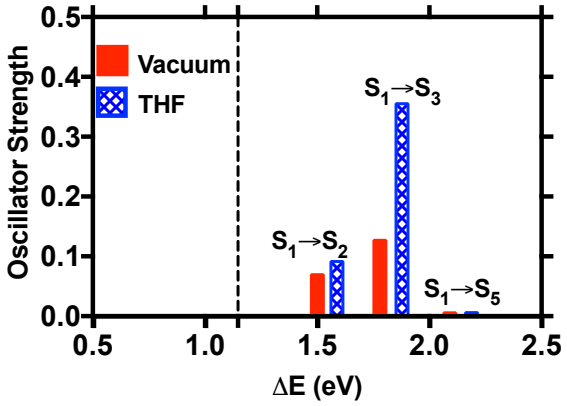

Figure S5: ESA peaks of 3MT trimer calculated in tetrahydrofuran (THF) (checkered blue) and vacuum (solid red). The vertical dashed line indicates the experimental ESA energy of P3HT.[19]

Oligomer Length Dependence

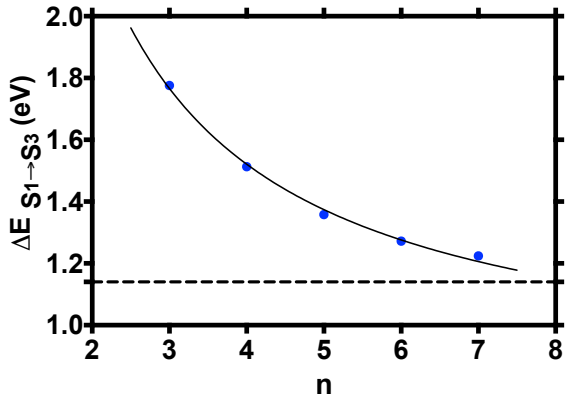

Figure S6: Calculated excitation energy of the $S_1 \rightarrow S_3$ transition for 3MT oligomers of length $n = 3$ to 7 obtained from the relaxed S_1 molecular geometry (blue data points). The solid curve shows the $1/n$ dependence of the excitation energy. The horizontal dashed line indicates the experimental ESA energy of P3HT.[19]

Electron Density Differences

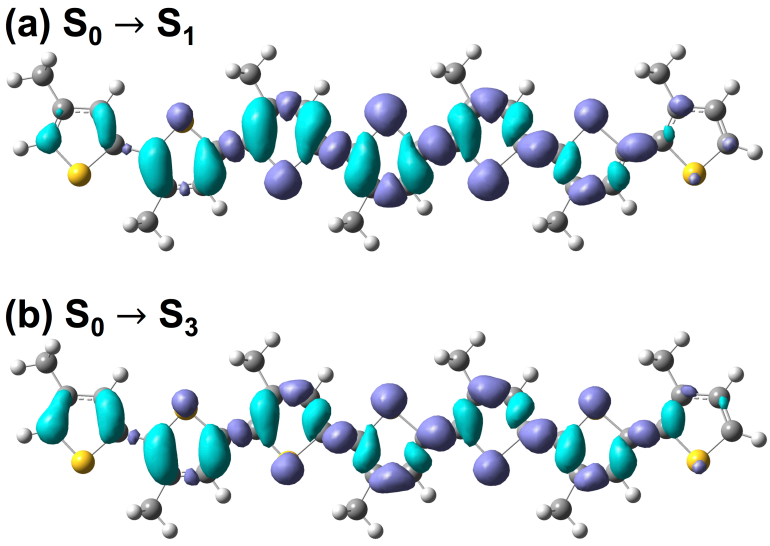

Figure S7: The electron density difference of 3MT heptamer at the S_1 geometry for the (a) $S_0 \rightarrow S_1$ and (b) $S_0 \rightarrow S_3$ transition, where the violet or turquoise colours represent the increase or decrease in electron density difference, respectively. The difference between the $S_0 \rightarrow S_3$ and $S_0 \rightarrow S_1$ transitions gives the electron density difference for the $S_1 \rightarrow S_3$ transition.

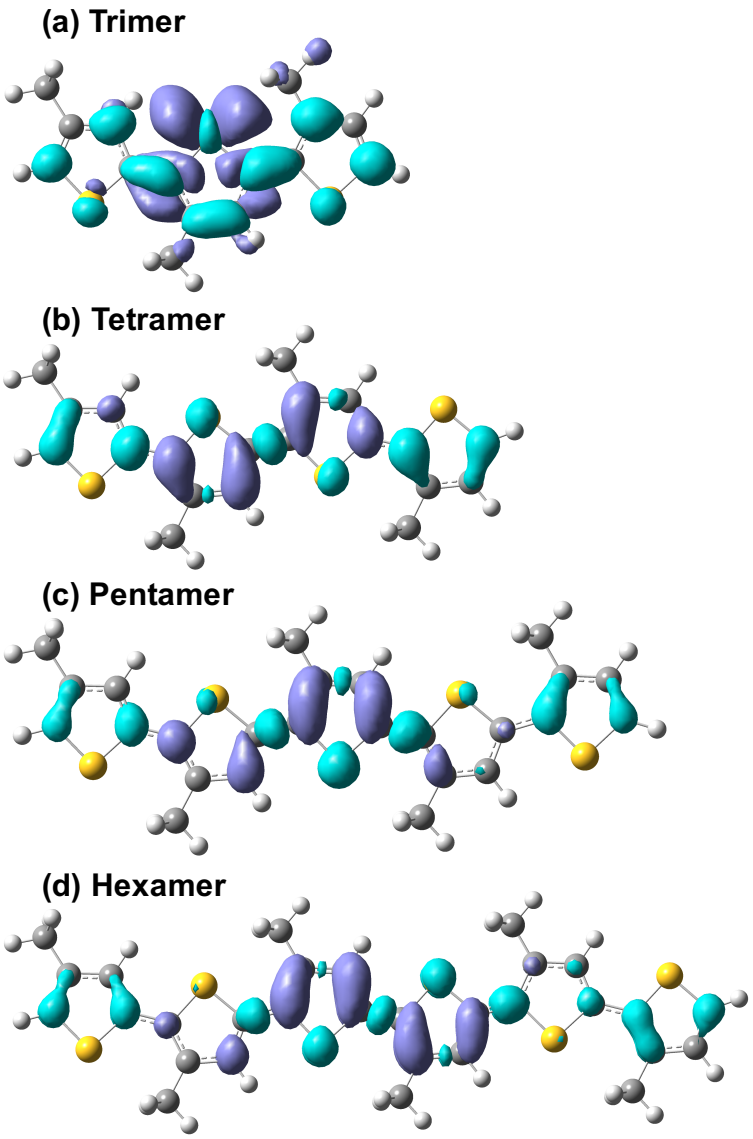

Figure S8: The electron density difference of 3MT (a) trimer, (b) tetramer, (c) pentamer and (d) hexamer for the $S_1 \rightarrow S_3$ transition, where the violet or turquoise colours represent the increase or decrease in electron density difference, respectively.

Natural Transition Orbitals

The nature of the $S_1 \rightarrow S_3$ transition is explored using natural transition orbitals (NTOs) and changes in electron density. In the NTO analysis, each transition is represented using a pair of orbitals, involving a transition to an excited "electron," leaving behind the empty "hole" (unoccupied).[3] In this case, the properties of the $S_1 \rightarrow S_3$ transition is inferred by examining the $S_0 \rightarrow S_1$ and $S_0 \rightarrow S_3$ transitions. Figure S9a shows the NTOs for the $S_0 \rightarrow S_1$ transition of the 3MT heptamer with a weighting of 92%. The $S_0 \rightarrow S_1$ transition has a negligible charge transfer character, as indicated by the similar orbital distribution between the "electron" and "hole." On the other hand, the NTOs for the $S_0 \rightarrow S_3$ transition of the 3MT heptamer cannot be represented by a single particle-hole transition. Two contributions with weightings of 58% (Figure S9b) and 40% (Figure S9c) must be considered. It is evident that the $S_0 \rightarrow S_3$ transition has a charge transfer character due to two complementary transfers of charge, i.e., from one side to the central part of the heptamer (Figure S9b) and from the central part to one side of the heptamer (Figure S9c). Although these two NTO contributions of the $S_0 \rightarrow S_3$ transition partially cancel out each other, this transition still maintain a charge-transfer character. Given that the $S_0 \rightarrow S_1$ transition has no charge-transfer character while the $S_0 \rightarrow S_3$ transition has one, it follows that the $S_1 \rightarrow S_3$ transition has a charge-transfer character.

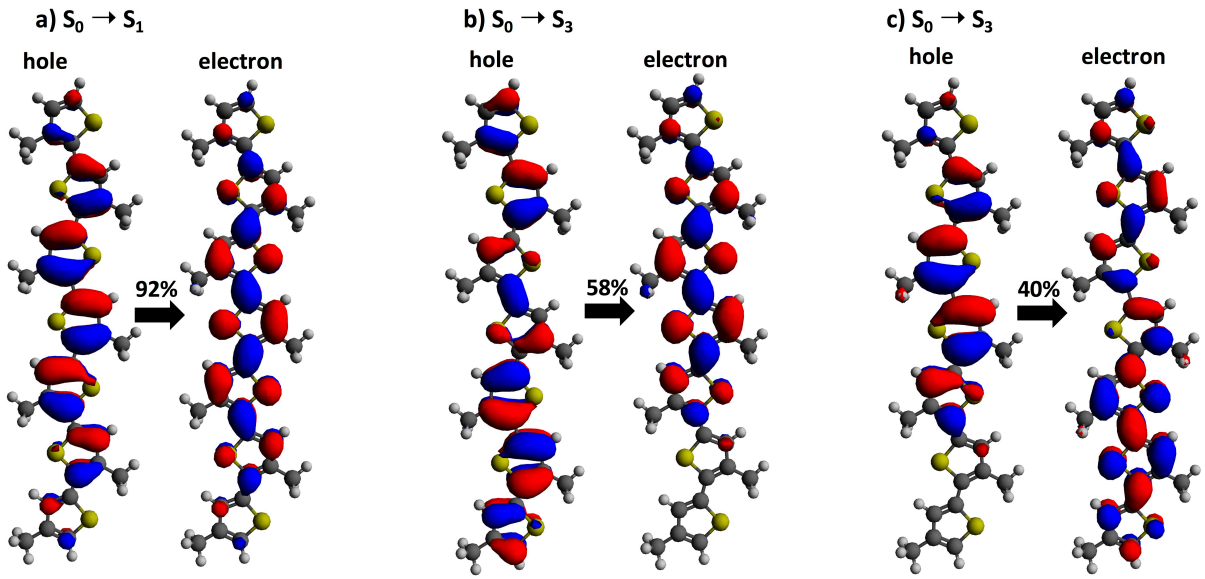

Figure S9: The electron–hole pairs of the natural transition orbital analysis for the $S_0 \rightarrow S_1$ and $S_0 \rightarrow S_3$ transitions of the heptamer at the S_1 geometry. The percentage value indicates the associated weighting of each pair of NTOs.

Dalton Parameters

Input commands used to perform the excited state absorption calculations using the Dalton2016 package.

```
**GENERAL
.RUN RESPONSE
.PARALLEL
.DIRECT
**WAVE FUNCTION
.DFT
 CAMB3LYP
**RESPONSE
*QUADRA
.PRINT LEVEL
 10
.DIPLEN
.DOUBLE RESIDUE
.ROOTS
 5
*END OF
```

Structure Coordinates

Table S1: Cartesian coordinates of S_0 and S_1 states of 3HT trimer.

3HT trimer S_0				3HT trimer S_1			
Atom	x	y	z	Atom	x	y	z
C	2.257 404	5.887 185	0.761 306	C	−1.857 438	6.216 627	0.038 660
C	1.201 598	5.668 843	−0.064 154	C	−0.634 154	5.924 272	0.582 214
C	0.874 456	4.284 737	−0.232 629	C	−0.320 525	4.551 846	0.631 265
C	1.712 235	3.470 947	0.491 535	C	−1.361 881	3.753 572	0.092 986
S	2.889 132	4.408 419	1.378 593	S	−2.695 594	4.793 908	−0.450 069
H	2.705 064	6.830 123	1.041 107	H	−2.312 149	7.187 756	−0.095 580
H	0.662 088	6.464 721	−0.564 745	H	0.040 048	6.688 968	0.951 679
C	1.762 390	2.016 546	0.606 601	C	−1.502 090	2.372 252	−0.058 690
C	2.876 164	1.227 369	0.683 862	C	−2.621 821	1.696 639	−0.629 766
S	0.331 665	1.041 007	0.764 687	S	−0.295 144	1.181 139	0.428 886
C	2.611 276	−0.166 213	0.845 582	C	−2.533 468	0.330 286	−0.694 400
H	3.880 204	1.629 540	0.607 308	H	−3.486 839	2.238 052	−0.994 764
C	1.263 976	−0.427 041	0.897 156	C	−1.294 609	−0.165 538	−0.160 780
C	−0.254 095	3.837 517	−1.121 445	C	0.998 354	4.060 857	1.154 610
H	−0.109 910	2.794 948	−1.418 690	H	0.878 441	3.120 088	1.700 943
H	−0.226 445	4.430 038	−2.043 252	H	1.368 239	4.786 972	1.886 758
C	3.716 393	−1.187 895	0.865 404	C	−3.655 160	−0.518 721	−1.224 323
H	4.439 668	−0.918 519	1.644 519	H	−4.262 820	0.098 358	−1.893 739
H	3.319 310	−2.168 101	1.137 846	H	−3.265 827	−1.335 934	−1.839 447

C	0.535 264	−1.687 635	1.030 348	C	−0.763 517	−1.453 141	−0.055 841
C	−0.549 077	−2.100 883	0.307 706	C	0.484 475	−1.801 204	0.499 337
S	0.907 261	−2.851 697	2.274 583	S	−1.568 199	−2.926 007	−0.617 988
C	−1.084 926	−3.361 329	0.722 779	C	0.770 269	−3.177 757	0.474 609
H	−0.949 192	−1.526 866	−0.520 621	H	1.159 245	−1.064 507	0.919 448
C	−0.387 325	−3.877 836	1.773 098	C	−0.246 950	−3.906 669	−0.097 519
H	−0.555 002	−4.819 169	2.278 105	H	−0.289 554	−4.978 305	−0.236 643
C	−2.276 400	−4.015 548	0.079 343	C	2.049 588	−3.781 251	0.986 804
H	−2.119 569	−4.069 445	−1.004 877	H	2.250 949	−3.398 794	1.994 340
H	−2.357 087	−5.048 356	0.433 648	H	1.926 772	−4.864 879	1.082 512
C	−3.592 896	−3.279 836	0.355 178	C	3.256 684	−3.483 625	0.089 208
H	−3.507 367	−2.240 539	0.014 758	H	3.372 708	−2.397 800	−0.012 912
H	−3.757 295	−3.235 200	1.438 616	H	3.056 340	−3.867 324	−0.918 491
C	−4.792 708	−3.938 541	−0.320 179	C	4.553 275	−4.088 129	0.620 803
H	−4.618 648	−3.984 261	−1.403 337	H	4.743 625	−3.705 418	1.632 172
H	−4.873 538	−4.979 579	0.019 330	H	4.431 336	−5.174 392	0.724 185
C	−6.109 978	−3.215 700	−0.050 325	C	5.762 056	−3.797 630	−0.265 219
H	−6.029 013	−2.174 267	−0.389 055	H	5.884 226	−2.711 222	−0.368 363
H	−6.284 237	−3.170 090	1.032 892	H	5.571 099	−4.179 274	−1.276 988
C	−7.311 970	−3.871 975	−0.725 744	C	7.061 072	−4.401 787	0.263 181
H	−7.392 010	−4.912 407	−0.387 104	H	6.938 083	−5.487 091	0.365 935
H	−7.137 026	−3.917 211	−1.807 842	H	7.250 910	−4.020 363	1.274 147
C	−8.623 579	−3.143 036	−0.450 518	C	8.263 286	−4.106 195	−0.628 287
H	−8.582 127	−2.109 322	−0.808 506	H	8.428 489	−3.028 042	−0.721 692
H	−9.466 787	−3.633 042	−0.945 167	H	9.178 984	−4.549 806	−0.227 683
H	−8.838 970	−3.111 752	0.622 360	H	8.113 192	−4.505 103	−1.636 639
C	−1.637 170	3.995 552	−0.476 535	C	2.067 237	3.880 223	0.063 435
H	−1.778 489	5.041 106	−0.176 480	H	2.214 019	4.837 952	−0.450 043
H	−1.676 658	3.405 056	0.446 974	H	1.699 533	3.176 647	−0.692 156
C	−2.772 464	3.570 828	−1.403 862	C	3.397 814	3.382 602	0.621 415
H	−2.723 599	4.159 537	−2.329 374	H	3.752 122	4.079 531	1.392 342
H	−2.625 024	2.524 009	−1.700 582	H	3.240 205	2.421 494	1.128 618
C	−4.155 395	3.728 355	−0.776 838	C	4.476 073	3.219 187	−0.446 944
H	−4.302 718	4.775 309	−0.480 191	H	4.634 818	4.180 624	−0.953 072
H	−4.203 748	3.140 458	0.149 348	H	4.120 249	2.524 310	−1.219 123
C	−5.293 145	3.303 107	−1.702 236	C	5.807 421	2.716 555	0.106 922
H	−5.243 731	3.890 452	−2.627 521	H	6.161 420	3.410 528	0.879 354
H	−5.145 253	2.257 052	−1.997 977	H	5.647 997	1.755 590	0.611 594
C	−6.671 131	3.464 550	−1.067 823	C	6.879 267	2.557 773	−0.967 031
H	−6.857 681	4.507 350	−0.791 778	H	7.081 162	3.511 165	−1.465 739
H	−7.466 526	3.153 602	−1.750 784	H	7.821 061	2.197 345	−0.544 077
H	−6.758 687	2.862 129	−0.157 959	H	6.564 258	1.844 280	−1.735 227
C	4.448 524	−1.300 631	−0.478 049	C	−4.560 259	−1.089 093	−0.121 973
H	4.846 759	−0.319 289	−0.762 771	H	−4.983 981	−0.255 133	0.449 955
H	3.726 652	−1.576 596	−1.256 193	H	−3.958 811	−1.673 668	0.583 239
C	5.584 421	−2.319 709	−0.446 362	C	−5.683 530	−1.960 030	−0.677 518
H	5.183 755	−3.301 023	−0.160 172	H	−5.248 274	−2.793 384	−1.244 727

H	6.298 850	−2.041 391	0.339 573	H	−6.273 588	−1.376 959	−1.396 787
C	6.320 807	−2.443 660	−1.777 873	C	−6.607 377	−2.513 352	0.404 520
H	6.721 509	−1.462 201	−2.064 263	H	−7.042 809	−1.679 999	0.971 628
H	5.606 095	−2.721 179	−2.563 971	H	−6.016 238	−3.094 900	1.124 309
C	7.458 029	−3.462 308	−1.749 923	C	−7.731 020	−3.388 214	−0.146 695
H	8.171 434	−3.184 548	−0.964 128	H	−8.320 973	−2.806 474	−0.865 776
H	7.056 940	−4.442 486	−1.463 668	H	−7.294 982	−4.220 092	−0.713 611
C	8.188 042	−3.579 202	−3.084 402	C	−8.648 731	−3.937 178	0.941 336
H	8.626 321	−2.620 174	−3.378 696	H	−9.122 668	−3.125 772	1.502 954
H	8.996 433	−4.314 062	−3.036 881	H	−9.443 504	−4.559 007	0.520 121
H	7.504 005	−3.887 345	−3.881 633	H	−8.089 586	−4.549 742	1.655 855

Table S2: Cartesian coordinates of S_0 and S_1 states of 3MT trimer.

3MT trimer S_0				3MT trimer S_1			
Atom	x	y	z	Atom	x	y	z
C	5.356 120	0.021 230	0.377 172	C	−5.359 231	−0.001 803	0.000 012
C	4.904 542	1.258 798	0.046 819	C	−4.871 705	1.280 439	0.000 005
C	3.491 840	1.320 619	−0.171 062	C	−3.468 586	1.377 734	−0.000 002
C	2.893 589	0.094 585	0.003 223	C	−2.850 580	0.101 276	−0.000 001
S	4.068 157	−1.119 533	0.447 261	S	−4.091 386	−1.167 719	0.000 009
H	6.370 601	−0.289 278	0.582 125	H	−6.391 406	−0.321 663	0.000 018
H	5.551 728	2.122 087	−0.055 111	H	−5.517 247	2.151 417	0.000 005
C	1.499 276	−0.306 169	−0.128 311	C	−1.508 358	−0.276 185	−0.000 005
C	1.016 282	−1.534 607	−0.490 343	C	−1.004 458	−1.612 842	−0.000 006
S	0.178 690	0.758 864	0.255 516	S	−0.154 892	0.857 839	−0.000 006
C	−0.404 102	−1.642 768	−0.486 911	C	0.359 434	−1.737 199	−0.000 008
H	1.662 351	−2.354 734	−0.782 589	H	−1.667 360	−2.469 997	−0.000 007
C	−1.007 539	−0.465 198	−0.112 607	C	1.028 920	−0.467 391	−0.000 006
C	2.797 855	2.595 622	−0.557 852	C	−2.747 880	2.691 326	−0.000 009
H	1.983 829	2.419 310	−1.264 015	H	−2.108 836	2.812 837	0.880 912
H	2.371 380	3.103 932	0.313 196	H	−2.108 835	2.812 828	−0.880 931
H	3.505 912	3.285 504	−1.021 770	H	−3.467 300	3.512 370	−0.000 014
C	−1.110 060	−2.908 259	−0.882 376	C	1.057 893	−3.062 978	−0.000 014
H	−1.369 112	−3.514 529	−0.008 320	H	1.694 214	−3.185 886	−0.881 407
H	−2.035 486	−2.704 839	−1.424 849	H	1.694 216	−3.185 894	0.881 377
H	−0.467 173	−3.516 813	−1.521 715	H	0.326 458	−3.872 698	−0.000 017
C	−2.417 515	−0.113 205	−0.005 238	C	2.384 004	−0.134 323	−0.000 003
C	−2.986 449	1.115 338	−0.207 489	C	2.931 446	1.163 576	−0.000 004
S	−3.630 668	−1.257 536	0.507 363	S	3.703 745	−1.314 360	0.000 008
C	−4.394 407	1.156 730	0.034 874	C	4.337 418	1.201 178	0.000 003
H	−2.417 088	1.976 788	−0.538 278	H	2.314 882	2.054 833	−0.000 012
C	−4.870 425	−0.059 010	0.423 883	C	4.888 835	−0.058 664	0.000 010
C	−5.232 181	2.389 734	−0.135 610	C	5.143 520	2.467 332	0.000 004
H	−5.179 057	2.763 676	−1.162 432	H	4.917 172	3.075 449	0.880 584
H	−6.279 596	2.190 659	0.098 185	H	6.214 060	2.255 449	−0.000 004
H	−4.885 763	3.194 759	0.519 349	H	4.917 159	3.075 458	−0.880 566

H	−5.892 353	−0.325 880	0.654 948	H	5.939 306	−0.315 510	0.000 016

Table S3: Cartesian coordinates of S_0 and S_1 states of 3MT tetramer.

3MT tetramer S_0				3MT tetramer S_1			
Atom	x	y	z	Atom	x	y	z
C	−7.247 213	−0.470 533	−0.625 704	C	−7.305 297	−0.363 563	−0.000 014
C	−6.933 807	0.840 913	−0.462 288	C	−6.918 471	0.945 433	−0.000 008
C	−5.553 322	1.073 871	−0.167 863	C	−5.515 870	1.141 353	−0.000 001
C	−4.837 468	−0.099 253	−0.112 914	C	−4.816 694	−0.073 436	−0.000 001
S	−5.862 206	−1.476 027	−0.437 204	S	−5.950 059	−1.425 563	−0.000 011
H	−8.211 318	−0.906 923	−0.844 046	H	−8.308 689	−0.764 466	−0.000 021
H	−7.660 638	1.641 406	−0.535 957	H	−7.623 171	1.768 971	−0.000 009
C	−3.427 770	−0.335 864	0.166 289	C	−3.430 063	−0.347 330	0.000 004
C	−2.867 526	−1.441 701	0.746 850	C	−2.823 853	−1.620 753	0.000 003
S	−2.181 313	0.783 087	−0.301 489	S	−2.186 209	0.891 394	0.000 009
C	−1.447 679	−1.409 467	0.846 361	C	−1.446 982	−1.637 200	0.000 006
H	−3.459 398	−2.267 652	1.124 647	H	−3.410 803	−2.532 198	0.000 001
C	−0.922 372	−0.248 065	0.327 296	C	−0.886 534	−0.318 276	0.000 009
C	−5.006 993	2.454 322	0.061 445	C	−4.897 975	2.507 654	0.000 007
H	−4.234 249	2.464 663	0.832 869	H	−4.270 489	2.676 095	0.881 136
H	−4.565 628	2.870 688	−0.850 039	H	−4.270 483	2.676 102	−0.881 117
H	−5.806 414	3.129 910	0.372 874	H	−5.677 627	3.271 537	0.000 007
C	−0.665 995	−2.525 819	1.477 822	C	−0.645 961	−2.903 228	0.000 006
H	−0.220 754	−3.183 343	0.724 155	H	−0.001 646	−2.977 902	−0.881 369
H	0.145 854	−2.150 576	2.104 912	H	−0.001 646	−2.977 903	0.881 381
H	−1.319 095	−3.139 740	2.100 981	H	−1.311 370	−3.768 130	0.000 005
C	0.453 148	0.219 451	0.253 177	C	0.426 746	0.120 102	0.000 008
C	0.889 129	1.516 466	0.194 497	C	0.866 877	1.473 625	0.000 006
S	1.810 033	−0.865 157	0.141 411	S	1.841 574	−0.938 582	0.000 006
C	2.298 046	1.667 839	0.054 989	C	2.233 452	1.655 194	0.000 004
H	0.216 108	2.364 557	0.250 808	H	0.169 417	2.302 763	0.000 007
C	2.943 029	0.454 448	0.005 883	C	2.950 642	0.432 610	0.000 003
C	4.358 880	0.136 043	−0.124 728	C	4.340 813	0.167 931	−0.000 001
C	4.910 935	−0.966 271	−0.719 736	C	4.953 970	−1.082 756	0.000 003
S	5.612 092	1.130 549	0.571 659	S	5.581 250	1.418 770	−0.000 013
C	6.336 267	−1.027 085	−0.634 832	C	6.368 443	−1.043 295	−0.000 003
H	4.315 658	−1.718 691	−1.225 078	H	4.392 126	−2.009 817	0.000 012
C	6.842 840	0.046 235	0.034 258	C	6.842 654	0.241 273	−0.000 012
C	2.951 634	3.017 834	−0.026 567	C	2.863 666	3.016 488	0.000 002
H	3.298 137	3.357 561	0.954 858	H	3.492 678	3.170 887	0.881 411
H	3.815 314	3.011 049	−0.694 277	H	3.492 673	3.170 889	−0.881 410
H	2.241 392	3.760 502	−0.395 951	H	2.092 263	3.788 158	0.000 005
C	7.158 643	−2.133 914	−1.226 335	C	7.238 761	−2.266 002	0.000 000
H	8.223 376	−1.973 943	−1.047 091	H	8.296 841	−1.998 388	−0.000 002
H	6.884 117	−3.101 540	−0.795 791	H	7.045 156	−2.885 606	0.880 504
H	7.003 818	−2.205 909	−2.307 004	H	7.045 153	−2.885 611	−0.880 501

H	7.881 596	0.272 054	0.231 669	H	7.874 796	0.563 354	−0.000 018

Table S4: Cartesian coordinates of S_0 and S_1 states of 3MT pentamer.

3MT pentamer S_0				3MT pentamer S_1			
Atom	x	y	z	Atom	x	y	z
C	9.263 004	0.152 276	0.310 431	C	−9.266 626	0.049 491	−0.000 012
C	8.825 717	1.046 185	−0.613 979	C	−8.784 928	1.323 146	0.000 021
C	7.409 555	1.025 008	−0.814 632	C	−7.365 889	1.409 398	0.000 031
C	6.793 623	0.089 462	−0.016 273	C	−6.767 520	0.152 393	0.000 005
S	7.957 376	−0.745 696	0.983 560	S	−7.992 891	−1.108 459	−0.000 033
H	10.276 508	−0.033 745	0.635 742	H	−10.296 547	−0.277 215	−0.000 026
H	9.485 331	1.709 830	−1.160 705	H	−9.423 624	2.198 661	0.000 039
C	5.389 541	−0.280 173	0.096 959	C	−5.391 790	−0.227 709	0.000 004
C	4.875 855	−1.493 922	0.466 943	C	−4.881 977	−1.527 724	0.000 001
S	4.096 945	0.855 935	−0.159 148	S	−4.069 343	0.917 393	0.000 001
C	3.455 974	−1.540 428	0.556 318	C	−3.498 206	−1.638 176	−0.000 003
H	5.500 110	−2.355 669	0.674 062	H	−5.527 516	−2.398 769	0.000 003
C	2.881 115	−0.328 668	0.247 139	C	−2.857 191	−0.370 534	−0.000 005
C	1.484 692	0.074 905	0.206 179	C	−1.508 340	−0.023 055	−0.000 009
C	0.982 104	1.341 965	0.341 413	C	−0.975 250	1.293 279	−0.000 015
S	0.188 463	−1.043 357	−0.109 893	S	−0.179 144	−1.180 930	−0.000 005
C	−0.429 015	1.445 642	0.191 714	C	0.395 182	1.387 024	−0.000 016
H	1.608 075	2.202 280	0.549 600	H	−1.615 389	2.167 785	−0.000 019
C	−1.009 773	0.224 301	−0.064 684	C	1.034 106	0.108 771	−0.000 010
C	−2.401 722	−0.137 249	−0.280 499	C	2.382 131	−0.244 142	−0.000 006
C	−2.882 819	−1.210 963	−0.981 832	C	2.910 579	−1.551 773	0.000 004
S	−3.724 099	0.750 461	0.420 534	S	3.717 586	0.905 874	−0.000 011
C	−4.301 081	−1.334 151	−0.987 484	C	4.297 868	−1.635 691	0.000 008
H	−2.237 241	−1.899 688	−1.515 131	H	2.276 636	−2.430 584	0.000 008
C	−4.906 654	−0.326 688	−0.273 134	C	4.917 547	−0.376 020	0.000 001
C	−6.316 724	−0.040 170	−0.044 736	C	6.298 654	−0.009 491	0.000 003
C	−6.896 906	1.185 412	0.144 228	C	6.820 997	1.272 269	−0.000 015
S	−7.514 231	−1.299 524	0.110 856	S	7.614 753	−1.172 893	0.000 030
C	−8.300 930	1.135 502	0.406 133	C	8.239 778	1.330 796	−0.000 007
H	−6.338 840	2.113 102	0.083 743	H	6.198 451	2.159 876	−0.000 034
C	−8.762 666	−0.146 231	0.412 833	C	8.797 377	0.083 613	0.000 018
C	6.728 595	1.928 483	−1.802 839	C	−6.647 197	2.726 354	0.000 069
H	5.910 277	1.423 886	−2.321 052	H	−6.009 209	2.845 993	0.881 370
H	6.310 754	2.816 619	−1.317 447	H	−6.009 226	2.846 053	−0.881 236
H	7.442 567	2.274 101	−2.553 210	H	−7.366 765	3.546 976	0.000 103
C	2.722 243	−2.791 766	0.946 044	C	−2.791 561	−2.959 693	−0.000 005
H	1.889 449	−2.582 010	1.621 044	H	−2.154 329	−3.081 864	−0.881 341
H	2.313 762	−3.309 721	0.072 247	H	−2.154 328	−3.081 867	0.881 329
H	3.398 804	−3.485 255	1.449 133	H	−3.517 816	−3.774 231	−0.000 006
C	−1.148 550	2.758 981	0.308 969	C	1.119 618	2.699 310	−0.000 024
H	−1.945 523	2.853 842	−0.431 736	H	1.758 011	2.809 735	0.881 501

H	−1.602 812	2.884 303	1.297 137	H	1.758 008	2.809 726	−0.881 552
H	−0.450 697	3.585 896	0.163 793	H	0.404 582	3.523 520	−0.000 026
C	−5.004 815	−2.436 195	−1.726 699	C	5.017 609	−2.952 733	0.000 020
H	−5.253 345	−3.270 913	−1.063 347	H	5.655 511	−3.065 478	−0.881 334
H	−5.936 007	−2.090 893	−2.180 361	H	5.655 500	−3.065 469	0.881 382
H	−4.365 151	−2.829 426	−2.519 434	H	4.299 651	−3.774 396	0.000 019
C	−9.149 362	2.352 577	0.629 965	C	9.021 503	2.611 701	−0.000 026
H	−10.191 851	2.080 391	0.804 618	H	10.095 777	2.418 977	0.000 016
H	−8.798 589	2.923 359	1.494 949	H	8.785 160	3.216 459	−0.880 501
H	−9.113 958	3.022 232	−0.234 513	H	8.785 102	3.216 520	0.880 391
H	−9.778 897	−0.482 172	0.565 452	H	9.848 143	−0.170 974	0.000 029

Table S5: Cartesian coordinates of S_0 and S_1 states of 3MT hexamer.

3MT hexamer S_0				3MT hexamer S_1			
Atom	x	y	z	Atom	x	y	z
C	11.217 629	0.132 386	0.007 333	C	11.220 428	0.180 360	−0.000 129
C	10.750 522	0.685 485	−1.141 933	C	10.780 143	−1.106 363	−0.000 062
C	9.327 999	0.621 034	−1.278 523	C	9.361 151	−1.235 008	−0.000 007
C	8.738 169	0.003 130	−0.200 571	C	8.728 543	−0.001 060	−0.000 035
S	9.934 004	−0.480 649	0.977 193	S	9.909 934	1.296 236	−0.000 131
H	12.241 533	0.046 798	0.341 865	H	12.239 129	0.540 461	−0.000 177
H	11.392 481	1.126 841	−1.895 288	H	11.444 788	−1.962 243	−0.000 048
C	7.337 690	−0.289 507	0.072 013	C	7.332 645	0.338 531	−0.000 001
C	6.832 663	−1.320 346	0.817 733	C	6.782 951	1.612 100	0.000 028
S	6.042 528	0.734 497	−0.476 154	S	6.053 112	−0.849 264	−0.000 007
C	5.417 138	−1.312 479	0.967 611	C	5.386 309	1.670 181	0.000 047
H	7.460 195	−2.086 690	1.258 289	H	7.394 245	2.507 457	0.000 039
C	4.837 120	−0.245 808	0.319 170	C	4.800 128	0.389 701	0.000 030
C	3.442 171	0.148 403	0.204 884	C	3.452 484	−0.009 647	0.000 037
C	2.950 799	1.402 500	−0.044 832	C	2.966 641	−1.333 670	0.000 019
S	2.129 876	−0.990 871	0.303 520	S	2.093 562	1.103 755	0.000 063
C	1.535 402	1.477 483	−0.166 447	C	1.595 637	−1.474 956	0.000 022
H	3.587 996	2.274 425	−0.139 643	H	3.633 949	−2.187 892	0.000 003
C	0.939 190	0.247 087	−0.005 212	C	0.917 382	−0.219 239	0.000 044
C	−0.461 767	−0.139 432	−0.045 688	C	−0.437 955	0.089 333	0.000 047
C	−0.973 346	−1.380 527	−0.319 226	C	−1.007 923	1.387 086	0.000 069
S	−1.755 338	0.960 593	0.337 786	S	−1.737 601	−1.102 478	0.000 023
C	−2.389 379	−1.478 614	−0.223 167	C	−2.386 044	1.436 549	0.000 065
H	−0.350 484	−2.225 068	−0.591 439	H	−0.396 107	2.281 525	0.000 085
C	−2.965 035	−0.280 179	0.132 945	C	−2.980 983	0.148 671	0.000 039
C	−4.359 646	0.076 046	0.341 287	C	−4.331 111	−0.245 674	0.000 022
C	−4.850 100	1.090 009	1.120 500	C	−4.823 447	−1.554 582	−0.000 002
S	−5.670 758	−0.729 377	−0.473 004	S	−5.687 968	0.871 036	0.000 022
C	−6.264 516	1.246 193	1.078 443	C	−6.218 112	−1.670 855	−0.000 021
H	−4.213 162	1.725 633	1.725 301	H	−4.171 855	−2.420 547	−0.000 007
C	−6.858 296	0.326 836	0.245 772	C	−6.858 601	−0.432 196	−0.000 013

C	−8.260 440	0.118 047	−0.091 072	C	−8.255 915	−0.091 875	−0.000 032
C	−8.769 540	−0.362 653	−1.267 379	C	−8.804 333	1.173 291	−0.000 082
S	−9.550 235	0.390 173	1.052 087	S	−9.540 958	−1.284 914	0.000 018
C	−10.190 836	−0.511 861	−1.274 169	C	−10.227 082	1.200 364	−0.000 081
H	−8.146 224	−0.593 948	−2.124 005	H	−8.202 637	2.075 263	−0.000 124
C	−10.737 882	−0.136 778	−0.084 050	C	−10.754 441	−0.057 990	−0.000 029
C	8.614 870	1.165 259	−2.483 426	C	8.684 260	−2.574 520	0.000 072
H	7.767 758	0.540 038	−2.773 459	H	8.050 611	−2.713 609	0.881 469
H	8.230 759	2.174 816	−2.303 806	H	8.050 631	−2.713 724	−0.881 322
H	9.298 717	1.224 424	−3.332 663	H	9.429 171	−3.372 126	0.000 132
C	4.692 626	−2.369 372	1.751 282	C	4.636 157	2.968 147	0.000 084
H	3.891 618	−1.946 346	2.361 736	H	3.995 348	3.069 251	−0.881 297
H	4.242 681	−3.121 882	1.095 607	H	3.995 357	3.069 206	0.881 477
H	5.385 832	−2.888 650	2.415 755	H	5.334 761	3.806 476	0.000 102
C	0.826 025	2.773 254	−0.438 088	C	0.916 993	−2.811 178	0.000 005
H	0.018 882	2.650 980	−1.163 941	H	0.282 640	−2.944 676	0.881 459
H	0.387 000	3.192 577	0.472 938	H	0.282 634	−2.944 651	−0.881 448
H	1.526 295	3.511 958	−0.832 549	H	1.660 046	−3.610 273	−0.000 009
C	−3.120 343	−2.763 432	−0.489 715	C	−3.146 231	2.729 403	0.000 085
H	−3.935 509	−2.922 214	0.219 749	H	−3.787 224	2.822 063	−0.881 479
H	−3.552 681	−2.781 214	−1.495 358	H	−3.787 246	2.822 023	0.881 637
H	−2.435 933	−3.610 582	−0.414 053	H	−2.454 109	3.572 892	0.000 114
C	−6.974 529	2.307 616	1.869 359	C	−6.904 044	−3.006 318	−0.000 049
H	−7.836 406	2.706 678	1.331 026	H	−7.538 856	−3.136 173	0.881 244
H	−7.336 343	1.921 498	2.827 816	H	−7.538 887	−3.136 120	−0.881 328
H	−6.295 872	3.134 958	2.086 924	H	−6.165 514	−3.809 597	−0.000 086
C	−10.970 121	−1.007 224	−2.456 781	C	−11.035 953	2.464 210	−0.000 134
H	−12.040 040	−1.032 010	−2.242 218	H	−12.105 839	2.248 317	−0.000 126
H	−10.813 923	−0.365 249	−3.328 828	H	−10.812 898	3.074 176	0.880 260
H	−10.657 656	−2.016 994	−2.739 234	H	−10.812 896	3.074 104	−0.880 577
H	−11.784 135	−0.125 971	0.188 321	H	−11.798 588	−0.338 297	−0.000 020

Table S6: Cartesian coordinates of S_0 and S_1 states of 3MT heptamer.

3MT heptamer S_0				3MT heptamer S_1			
Atom	x	y	z	Atom	x	y	z
C	13.167 413	0.179 501	0.200 316	C	13.175 721	−0.066 361	0.020 624
C	12.731 557	0.507 179	−1.043 672	C	12.697 023	−1.338 130	0.006 056
C	11.313 211	0.412 157	−1.203 427	C	11.272 782	−1.421 973	−0.002 928
C	10.694 292	0.002 684	−0.045 344	C	10.681 127	−0.171 592	0.005 291
S	11.857 978	−0.248 328	1.233 016	S	11.899 141	1.088 186	0.024 522
H	14.181 925	0.162 179	0.571 876	H	14.204 688	0.263 138	0.029 392
H	13.393 607	0.803 836	−1.848 738	H	13.334 394	−2.214 428	0.001 269
C	9.286 958	−0.240 144	0.239 894	C	9.290 500	0.212 730	0.000 702
C	8.761 794	−1.108 734	1.158 418	C	8.780 439	1.496 149	−0.002 160
S	8.006 759	0.648 027	−0.534 024	S	7.979 067	−0.936 886	0.000 924
C	7.342 669	−1.080 893	1.264 751	C	7.378 378	1.590 386	−0.004 146

H	9.376 942	−1.770 089	1.757 880	H	9.414 366	2.375 547	−0.003 324
C	6.780 234	−0.165 397	0.404 380	C	6.764 990	0.333 315	−0.002 828
C	5.388 968	0.190 678	0.176 984	C	5.395 598	−0.033 592	−0.004 114
C	4.904 648	1.368 473	−0.327 867	C	4.874 905	−1.333 321	−0.003 750
S	4.074 546	−0.914 083	0.462 483	S	4.076 385	1.118 838	−0.005 450
C	3.493 227	1.410 379	−0.500 160	C	3.492 264	−1.432 081	−0.004 359
H	5.544 239	2.208 221	−0.574 911	H	5.513 629	−2.209 210	−0.003 063
C	2.892 728	0.232 459	−0.116 066	C	2.859 578	−0.161 701	−0.005 217
C	1.493 757	−0.162 322	−0.117 126	C	1.509 405	0.191 326	−0.005 642
C	0.990 201	−1.436 067	−0.147 210	C	0.981 505	1.504 520	−0.006 652
S	0.189 634	0.985 073	−0.003 219	S	0.177 818	−0.960 478	−0.004 462
C	−0.427 701	−1.521 169	−0.074 700	C	−0.392 019	1.601 488	−0.006 361
H	1.620 298	−2.314 828	−0.224 422	H	1.622 545	2.378 421	−0.007 569
C	−1.014 281	−0.278 459	0.013 173	C	−1.031 515	0.328 587	−0.005 033
C	−2.413 443	0.104 522	0.104 635	C	−2.383 597	−0.019 270	−0.003 949
C	−2.923 026	1.278 034	0.595 011	C	−2.917 393	−1.323 486	−0.002 430
S	−3.707 682	−0.898 155	−0.487 608	S	−3.711 407	1.136 932	−0.003 925
C	−4.337 050	1.401 854	0.502 384	C	−4.302 377	−1.404 596	−0.001 182
H	−2.300 392	2.054 623	1.024 549	H	−2.286 325	−2.204 450	−0.002 179
C	−4.914 162	0.292 653	−0.073 334	C	−4.920 483	−0.139 633	−0.001 725
C	−6.307 540	−0.010 244	−0.358 757	C	−6.291 155	0.227 277	−0.000 695
C	−6.792 769	−0.875 667	−1.303 113	C	−6.813 174	1.514 709	−0.001 207
S	−7.626 338	0.662 098	0.557 756	S	−7.612 837	−0.924 469	0.001 634
C	−8.208 697	−1.022 607	−1.308 933	C	−8.217 767	1.594 024	0.000 263
H	−6.151 064	−1.408 669	−1.995 629	H	−6.186 653	2.399 078	−0.002 580
C	−8.809 558	−0.248 197	−0.344 311	C	−8.819 085	0.342 823	0.001 968
C	−10.215 388	−0.083 575	0.001 235	C	−10.211 787	−0.039 216	0.003 942
C	−10.739 947	0.205 551	1.232 232	C	−10.723 937	−1.316 137	0.006 293
S	−11.488 753	−0.155 695	−1.189 564	S	−11.525 951	1.118 756	0.003 568
C	−12.160 109	0.364 862	1.242 255	C	−12.147 251	−1.382 174	0.007 825
H	−10.128 926	0.289 923	2.124 077	H	−10.098 354	−2.201 786	0.006 992
C	−12.690 693	0.191 792	−0.000 659	C	−12.707 360	−0.139 171	0.006 591
C	10.632 962	0.720 245	−2.506 838	C	10.555 302	−2.740 474	−0.019 929
H	9.800 214	0.041 511	−2.703 314	H	9.919 756	−2.872 250	0.861 175
H	10.235 274	1.740 313	−2.523 951	H	9.916 039	−2.847 582	−0.901 584
H	11.342 004	0.634 229	−3.332 760	H	11.275 468	−3.560 364	−0.032 752
C	6.597 654	−1.968 758	2.220 089	C	6.666 142	2.910 212	−0.007 853
H	5.779 937	−1.439 557	2.714 580	H	6.029 209	3.027 522	−0.889 932
H	6.166 420	−2.837 515	1.712 213	H	6.028 279	3.031 945	0.872 965
H	7.272 933	−2.344 019	2.991 376	H	7.388 493	3.728 138	−0.009 506
C	2.792 080	2.623 774	−1.040 503	C	2.775 849	−2.748 578	−0.004 157
H	2.005 831	2.357 268	−1.750 479	H	2.137 794	−2.864 470	0.877 242
H	2.327 701	3.211 486	−0.242 041	H	2.137 943	−2.864 814	−0.885 616
H	3.503 505	3.274 287	−1.552 665	H	3.495 709	−3.568 656	−0.003 924
C	−1.148 483	−2.838 696	−0.096 991	C	−1.111 033	2.916 959	−0.007 297
H	−1.954 816	−2.874 300	0.639 319	H	−1.749 428	3.029 159	−0.888 607
H	−1.590 826	−3.041 548	−1.077 634	H	−1.748 517	3.030 906	0.874 449

H	−0.454 565	−3.652 185	0.122 606	H	−0.392 772	3.738 338	−0.008 480
C	−5.064 451	2.621 375	0.991 949	C	−5.027 818	−2.718 037	0.000 616
H	−5.864 909	2.918 469	0.310 686	H	−5.665 290	−2.827 439	0.882 804
H	−5.515 630	2.455 120	1.975 518	H	−5.666 838	−2.829 008	−0.880 255
H	−4.373 066	3.460 711	1.088 040	H	−4.313 602	−3.542 931	0.000 732
C	−8.913 013	−1.931 482	−2.275 469	C	−8.936 864	2.912 178	0.000 013
H	−9.784 552	−2.408 347	−1.822 751	H	−9.575 398	3.026 280	−0.880 829
H	−9.259 155	−1.388 003	−3.160 579	H	−9.574 046	3.027 345	0.881 692
H	−8.235 721	−2.716 005	−2.619 259	H	−8.218 623	3.733 698	−0.001 044
C	−12.954 852	0.669 945	2.477 786	C	−12.920 559	−2.668 000	0.010 520
H	−14.020 757	0.741 150	2.253 833	H	−13.996 043	−2.481 917	0.011 304
H	−12.818 769	−0.107 011	3.235 955	H	−12.681 607	−3.272 938	−0.869 203
H	−12.638 590	1.616 791	2.925 543	H	−12.679 863	−3.270 290	0.891 584
H	−13.732 528	0.234 738	−0.286 428	H	−13.758 407	0.113 977	0.007 319

References

(1) Frisch, M. J.; Trucks, G. W.; Schlegel, H. B.; Scuseria, G. E.; Robb, M. A.; Cheeseman, J. R.; Scalmani, G.; Barone, V.; Mennucci, B.; Petersson, G. A. et al. Gaussian09 Revision E.01. Gaussian Inc. Wallingford CT 2009.

(2) Aidas, K.; Angeli, C.; Bak, K. L.; Bakken, V.; Bast, R.; Boman, L.; Christiansen, O.; Cimiraglia, R.; Coriani, S.; Dahle, P. et al. The Dalton Quantum Chemistry Program System. *WIREs Comput. Mol. Sci.* **2014**, *4*, 269–284.

(3) Martin, R. L. Natural Transition Orbitals. *J. Chem. Phys.* **2003**, *118*, 4775–4777.

(4) Lu, T.; Chen, F. Multiwfn: A Multifunctional Wavefunction Analyzer. *J. Comput. Chem.* **2012**, *33*, 580–592.

(5) Hanwell, M. D.; Curtis, D. E.; Lonie, D. C.; Vandermeersch, T.; Zurek, E.; Hutchison, G. R. Avogadro: An Advanced Semantic Chemical Editor, Visualization, and Analysis Platform. *J. Cheminf.* **2012**, *4*, 17.

(6) Dennington, R.; Keith, T.; Millam, J. GaussView Version 5. Semichem Inc. Shawnee Mission KS 2009.

(7) Reichenberger, M.; Love, J. A.; Rudnick, A.; Bagnich, S.; Panzer, F.; Stradomska, A.; Bazan, G. C.; Nguyen, T.-Q.; Köhler, A. The Effect of Intermolecular Interaction on Excited States in p-DTS(FBTTH$_2$)$_2$. *J. Chem. Phys.* **2016**, *144*, 74904.

(8) Casado, J.; Pappenfus, T. M.; Miller, L. L.; Mann, K. R.; Orti, E.; Viruela, P. M.; Pou-Amerigo, R.; Hernandez, V.; Lopez Navarrete, J. T. Nitro-functionalized Oligothiophenes as a Novel Type of Electroactive Molecular Material: Spectroscopic, Electrochemical, and Computational Study. *J. Am. Chem. Soc.* **2003**, *125*, 2524–2534.

(9) Irfan, A.; Al-Sehemi, A. G. DFT Study of the Electronic and Charge Transfer Properties of Perfluoroarene–thiophene Oligomers. *J. Saudi Chem. Soc.* **2014**, *18*, 574–580.

(10) Ling, S.; Schumacher, S.; Galbraith, I.; Paterson, M. J. Excited-State Absorption of Conjugated Polymers in the Near-Infrared and Visible: A Computational Study of Oligofluorenes. *J. Phys. Chem. C* **2013**, *117*, 6889–6895.

(11) Di Nuzzo, D.; Fontanesi, C.; Jones, R.; Allard, S.; Dumsch, I.; Scherf, U.; von Hauff, E.; Schumacher, S.; Da Como, E. How Intermolecular Geometrical Disorder Affects the Molecular Doping of Donor-acceptor Copolymers. *Nat. Commun.* **2015**, *6*, 6460.

(12) Bidan, G.; De Nicola, A.; Enée, V.; Guillerez, S. Synthesis and UV–visible Properties of Soluble Regioregular Oligo(3-octylthiophenes), Monomer to Hexamer. *Chem. Mater.* **1998**, *10*, 1052–1058.

(13) Gierschner, J.; Cornil, J.; Egelhaaf, H.-J. Optical Bandgaps of π-Conjugated Organic Materials at the Polymer Limit: Experiment and Theory. *Adv. Mater.* **2007**, *19*, 173–191.

(14) Barford, W.; Lidzey, D. G.; Makhov, D. V.; Meijer, A. J. H. Exciton Localization in Disordered Poly(3-hexylthiophene). *J. Chem. Phys.* **2010**, *133*, 044504.

(15) Yanai, T.; Tew, D. P.; Handy, N. C. A New Hybrid Exchange–correlation Functional using the Coulomb-attenuating Method (CAM-B3LYP). *Chem. Phys. Lett.* **2004**, *393*, 51 – 57.

(16) Paterson, M. J.; Christiansen, O.; Pawowski, F.; Jrgensen, P.; Httig, C.; Helgaker, T.; Saek, P. Benchmarking Two-photon Absorption with CC3 Quadratic Response Theory, and Comparison with Density-Functional Response Theory. *J. Chem. Phys.* **2006**, *124*, 054322.

(17) Chai, J.-D.; Head-Gordon, M. Systematic Optimization of Long-range Corrected Hybrid Density Functionals. *J. Chem. Phys.* **2008**, *128*, 084106.

(18) Chai, J.-D.; Head-Gordon, M. Long-range Corrected Hybrid Density Functionals with Damped Atom-atom Dispersion Corrections. *Phys. Chem. Chem. Phys.* **2008**, *10*, 6615–6620.

(19) Tapping, P. C.; Kee, T. W. Optical Pumping of Poly(3-hexylthiophene) Singlet Excitons Induces Charge Carrier Generation. *J. Phys. Chem. Lett.* **2014**, *5*, 1040–1047.

(20) Parkinson, P.; Muller, C.; Stingelin, N.; Johnston, M. B.; Herz, L. M. Role of Ultrafast Torsional Relaxation in the Emission from Polythiophene Aggregates. *J. Phys. Chem. Lett.* **2010**, *1*, 2788–2792.

(21) Busby, E.; Carroll, E. C.; Chinn, E. M.; Chang, L.; Moulé, A. J., A. J.e; Larsen, D. S. Excited-State Self-trapping and Ground-state Relaxation Dynamics in Poly(3-hexylthiophene) Resolved with Broadband Pump-dump-probe Spectroscopy. *J. Phys. Chem. Lett.* **2011**, *2*, 2764–2769.

(22) Kee, T. W. Femtosecond Pump-Push-Probe and Pump-Dump-Probe Spectroscopy of Conjugated Polymers: New Insight and Opportunities. *J. Phys. Chem. Lett.* **2014**, *5*, 3231–3240.

(23) Kraabel, B.; Moses, D.; Heeger, A. J. Direct Observation of the Intersystem Crossing in Poly(3-octylthiophene). *J. Chem. Phys.* **1995**, *103*, 5102–5108.

(24) Cook, S.; Furube, A.; Katoh, R. Analysis of the Excited States of Regioregular Polythiophene P3HT. *Energy Environ. Sci.* **2008**, *1*, 294–299.

(25) Yu, W.; Magnanelli, T. J.; Zhou, J.; Bragg, A. E. Structural Heterogeneity in the Localized Excited States of Poly(3-hexylthiophene). *J. Phys. Chem. B* **2016**, *120*, 5093–5102.

(26) Denis, J.-C.; Ruseckas, A.; Hedley, G. J.; Matheson, A. B.; Paterson, M. J.; Turnbull, G. A.; Samuel, I. D. W.; Galbraith, I. Self-trapping and Excited State Absorption in Fluorene Homopolymer and Copolymers with Benzothiadiazole and Tri-phenylamine. *Phys. Chem. Chem. Phys.* **2016**, *18*, 21937–21948.

(27) Salzner, U. Electronic Structure of Conducting Organic Polymers: Insights from Time-dependent Density Functional Theory. *WIREs Comput. Mol. Sci.* **2014**, *4*, 601–622.